Interpretation of
A Detailed Aeromagnetic Survey
and
Supplemental Geophysical Surveys
East Rift Zone, Hawaii

prepared for

THERMAL POWER COMPANY

601 CALIFORNIA STREET

SAN FRANCISCO, CALIFORNIA

by

HOWARD P. ROSS, PH.D.
Geophysical Consultant
Salt Lake City , Utah

NOVEMBER 1983

INTERPRETATION OF

A DETAILED AEROMAGNETIC SURVEY

AND

SUPPLEMENTAL GEOPHYSICAL SURVEYS

EAST RIFT ZONE, HAWAII

by

Howard P. Ross, Ph.D.
Consulting Geophysicist

October 1983

For

Thermal Power Company
601 California Street
San Francisco, CA 94108

CONTENTS

Page

INTRODUCTION.....1

GEOLOGY.....2

DETAILED AEROMAGNETIC SURVEY.....7

Survey Specifications and Statistics.....7
Data Compilation and Contractor Deliverables.....8

INTERPRETATION.....12

Procedures.....12
Interpretation Overview.....19

SUPPLEMENTAL GEOPHYSICAL DATA.....30

General Data Base.....30
ARCO Self Potential Survey.....31
ARCO Microearthquake Survey.....33
ARCO TDEM Survey.....35

DISCUSSION.....37

SUMMARY AND RECOMMENDATIONS.....41

REFERENCES.....44

APPENDIX I. NUMERICAL MODEL RESULTS.....46

LIST OF ILLUSTRATIONS

Figure 1 Generalized location map showing major geologic features of the east rift zone.

Figure 2 Generalized cross section from Mauna Kea to the Puna Ridge showing fresh and salt-water distribution.

Figure 3 Aeromagnetic Survey Area

Figure 4 Characteristic anomaly shapes, Hawaii magnetic field parameters.

Figure 5 Southeast coast dike numerical models.

Figure 6 Quarterly plot of earthquake epicenters, island of Hawaii, during 1963.

Figure 7 Quarterly plot of earthquake epicenters, island of Hawaii, during 1965.

Figure 8 Puu Kaliu Rift profile and numerical model.

Plate I Generalized Geology and Thermal Well Map, East Rift Area, Hawaii (1:100,000).

Plate II Composite Residual Magnetic Intensity, East Rift Area, Hawaii (1:100,000).

Plate III Aeromagnetic Interpretation, East Rift Area, Hawaii (1:100,000).

Plate IV ARCO Self Potential Survey, East Rift Area, Hawaii (1:100,000).

Plate V ARCO Microearthquake Survey, East Rift Area, Hawaii (1:100,000).

Plate VI ARCO Time Domain Electromagnetic (TDEM) Survey and Exploration Data Summary, Puna Geothermal Area, Hawaii (1:24,000).

Plate VII Interpreted Geologic Structure and Possible Reservoir Area, Puna Geothermal Area, Hawaii (1:24,000).

Plate VIII Interpreted Physical Property Cross Sections, Puna Geothermal Area, Hawaii (1:24,000).

INTRODUCTION

The drilling of the successful geothermal well HGP-A by the Hawaii Institute of Geophysics in 1976 culminated several years of regional and detailed geologic and geophysical studies in the Kilauea east rift zone on the island of Hawaii. A potential geothermal reservoir in the Puna District had been identified through a systematic exploration program conducted by the Hawaii Institute of Geophysics (HIG), the Colorado School of Mines (CSM) and the U.S. Geological Survey (USGS). Subsequent drilling by Thermal Power Company and its associates has resulted in two more potential producing wells and thus verified the presence of a major geothermal reservoir.

The extent of the geothermal reservoir and the geothermal potential of nearby areas within the east rift zone are now being evaluated by the Puna Geothermal Venture, a joint venture project of Thermal Power Company, Dillininghamand Puna Sugar. Thermal Power Company engaged Howard P. Ross as a consultant in exploration geophysics to compile, review and evaluate a large public geophysical data base as one part of the ongoing exploration effort. Ross (1982) noted that the Puna geothermal system was expressed in self-potential and resistivity data but was not well delineated by these or other data sets. Regional aeromagnetic data indicated a complex geologic structure for the east rift zone that was not apparent in other geophysical data or geologic maps. A detailed, low level aeromagnetic survey was recommended as a cost effective means to define subsurface structural features and hopefully the Puna geothermal reservoir. Ross (1982) postulated a major transverse fault may have localized the geothermal system within the east rift zone.

Dr. Ross was later retained as a consultant to interface with aeromagnetic survey contractors, to assist in the design of the detailed

survey and to complete a quantitative interpretation of the resulting data. In addition Ross was asked to review an extensive proprietary data base, the ARCO geophysical data, which was acquired by Thermal Power Company from Atlantic Richfield Corporation in January 1983. This report documents the aeromagnetic survey and its interpretation, and evaluates the ARCO data in the context of the aeromagnetic survey and the earlier geophysical compilation. The 1983 magnetic data provide a detailed, continuous data base to which all other survey data can be related.

GEOLOGY

A voluminous literature describes various aspects of the geology, petrology, volcanic and tectonic setting of the island of Hawaii and the Kilauea east rift zone. A detailed review of these data is beyond the scope of the present study. It is useful however to include a general description of the geologic setting from Ross (1982) as a background to later geophysical discussions.

Kilauea Volcano is the southeasternmost shield volcano in the Hawaiian-Emperor chain of islands. Kilauea, situated on the east flank of Mauna Loa, (Figure 1) and Mauna Loa itself, are among the most active volcanoes on earth (Swanson et al., 1976). The east rift extends from Kilauea southeastward for 7.3 km, then trends N65°E past Cape Kumukahi where it can be traced by bathymetry for approximately 70 km (Moore, 1971). The geology of the entire eastern portion of the island of Hawaii is dominated by a great sequence of seaward dipping lava flows which emanate from Mauna Loa and Kilauea Volcanoes. The younger flows fill in earlier vents and flow features and obscure older faults, fissures, and entire flow systems. Geologic studies by Peterson (1967), and Moore (1971) indicate the geologic structure and extent

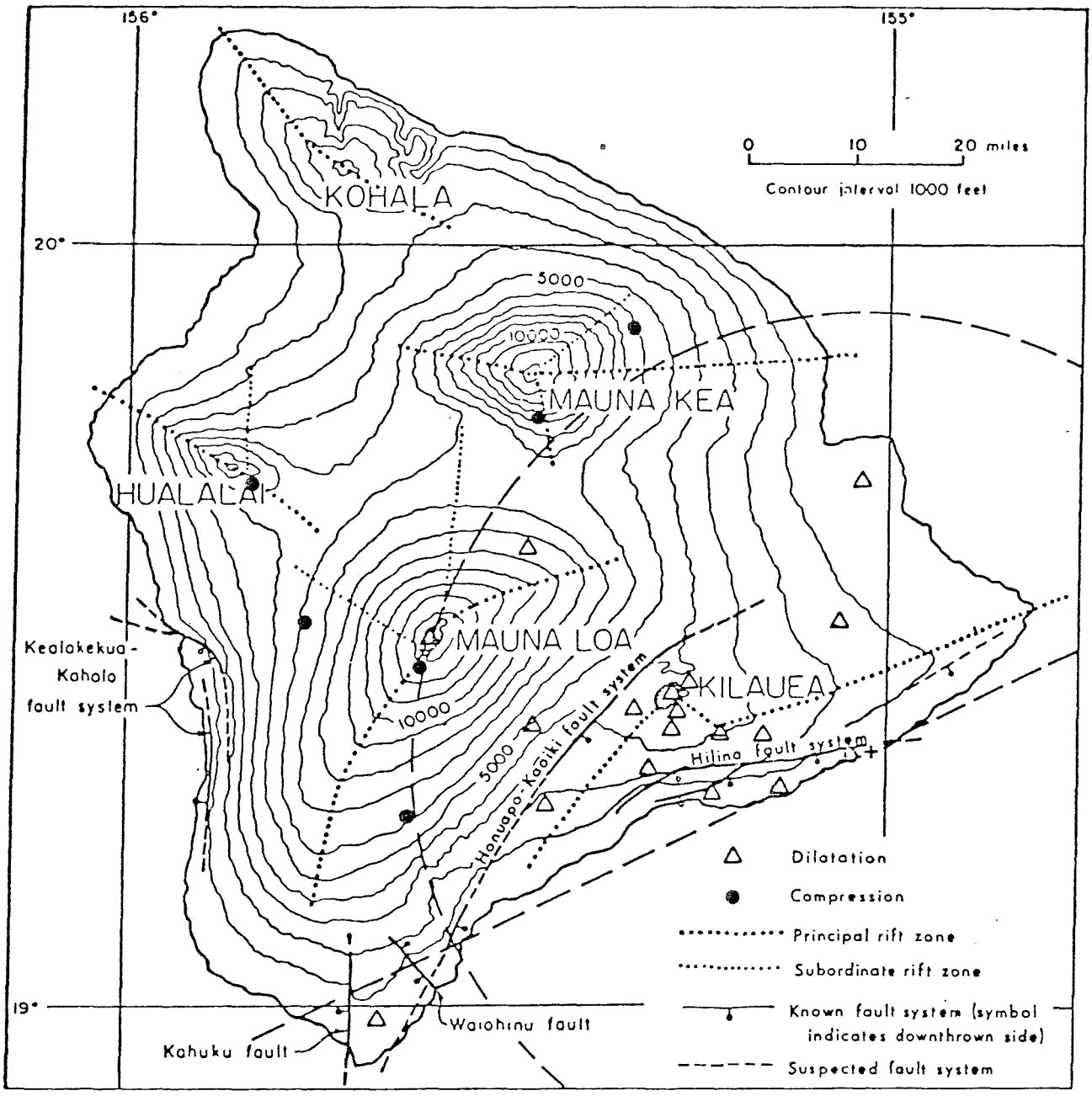

Fig. 1. Generalized location map showing major geologic features in relation to the Kilauea east rift zone. The distribution of dilations and compressions as determined by the seismic stations of the Hawaiian Volcano Observatory are also indicated. (From Furumoto and Kovach, 1979).

of historical flows in the Kilauea and east rift areas. Holcomb (1980) and Moore (1982) present detailed geologic mapping of lava flows, fissures and faulting for the Kilauea and east rift zones. The principal geologic features of Holcomb's (1980) map, reduced to 1:100,000 scale, is presented as Plate I of this report. The petrography of the volcanic rocks is described by Macdonald (1949) who noted that the lavas of Mauna Loa and Kilauea Volcanoes are predominantly olivine basalt with smaller proportions of basalt.

The subsurface structure and tectonic setting of the east rift area, of prime importance to the evaluation of geothermal resource potential, has been studied through integrated geologic, seismic and gravity studies (Furumoto and Kovach, 1979; Swanson et al., 1976). Seismic evidence in particular indicates that the southeast side of the rift zone is being displaced seaward by the intrusion of magma as dikes within the rift zone. The dikes are believed to be individually thin, a few meters wide, and to be nearly vertical or to dip steeply southward (Swanson et al., 1976). The north flank of the rift zone is relatively immobile and less seismically active. This results from the buttressed position of Kilauea and the rift zone itself, against the stable south flank of the massive Mauna Loa shield volcano, in marked contrast to the unbounded south flank. Swanson et al. (1976) suggest that the active seaward side of the rift zone has probably migrated several kilometers eastward in recent time. Triangulation, trilateration and leveling data indicate the south flank of Kilauea has been displaced upward and away from the rift zone by several meters during the 20th century alone. Keller et al. (1977) point out that grabens bounding the rift zone have been filled repeatedly, making vertical movement within the graben difficult to measure.

The high rainfall in the eastern Hawaii area (100-200 inches/yr) produces

ground waters which move readily through the porous and permeable basalts and move down dip relatively unimpeded until ponded by the dikes and structures of the east rift zone (Fig. 2). Thus a typical Ghyben-Herzberg system probably is not present in the east rift area of Hawaii (Keller et al., 1977). Both electrical resistivity data and drill results indicate salt water close to sea level in the Puna area.

The principal faults, fissures and caldera features of the east rift zone (Holcomb, 1980) are shown in Plate I which is intended to serve as a simplified geologic base map for this report. The details of the flow sequences have been omitted since they seem to bear relatively little detailed relationship to the geophysical data at this scale.

1983 Volcanic Activity

A major period of eruptive activity within the east rift zone of Kilauea Volcano began on January 3, 1983 and has continued intermittently through July. The eruptions began at Napau Crater, 14 km southeast of the Kilauea caldera rim, within the southwestern portion of the aeromagnetic survey and the area covered by ARCO self-potential (SP) and microearthquake data. Active vents migrated at least 6 km downrift (NE) resulting in strong fountaining (400 feet into the air) and extensive lava production. After a period of near continuous activity in January the rift zone became quiescent only to become intermittently active with occassional strong fountaining and extensive lava production. Major flow activity accompanied by swarm earthquake activity and occassional harmonic tremors occurred as late as July 1983 (USGS Hawaiian Volcano Observatory, 1983). The magnitude of the eruptive activity, and its occurrence during the aeromagnetic survey emphasize the ongoing nature of volcanic processes within the study area. These processes are active to a

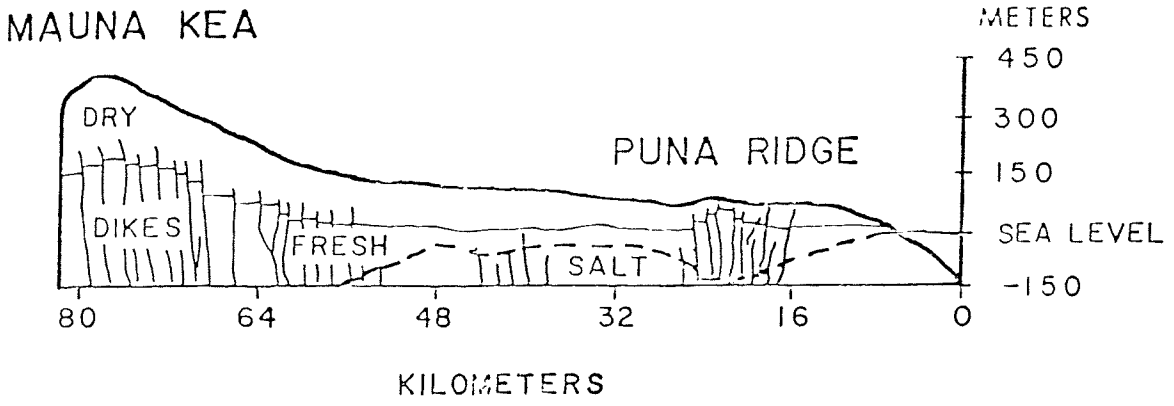

Figure 2a Generalized cross-section from Mauna Kea to the Puna Ridge showing fresh and salt-water distribution (after Stearns and Macdonald, 1946, p. 225).

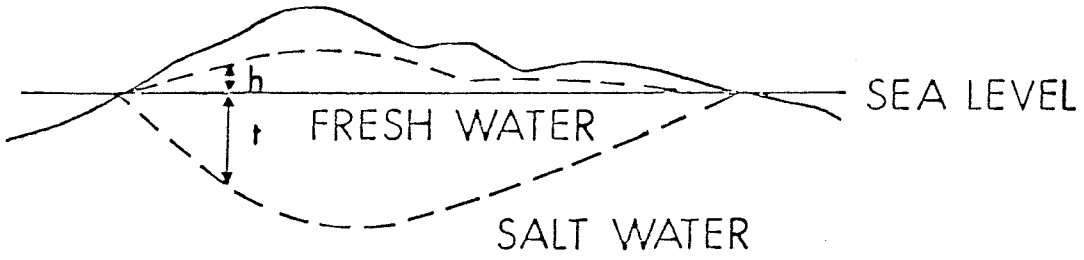

Figure 2b The Ghyben-Herzberg Principle showing the lens of fresh water depressed below sea level (after Stearns, 1966, p. 234).

Figures 2a and 2b taken from Keller et al., 1977.

degree which can modify the geophysical data base during our period of exploration and evaluation.

DETAILED AEROMAGNETIC SURVEY

Initial attempts to obtain a proprietary aeromagnetic survey of the Kilauea east rift zone resulted in high cost estimates and disinterest on the part of several major geophysical contractors. The remote location and relatively small survey size resulted in cost estimates ranging from $56,000 to $92,500 (plus $17,000/day standby charges). It was decided to await the through transit of a U.S. contractor aircraft working in the Pacific, or to contract with the Earth Science Laboratory/UURI, for a "button on" aeromagnetic survey using a local aircraft. A contract was ultimately negotiated with Geometrics in January, 1983 to complete a state-of-the-art survey using a Beechcraft Queen Aire aircraft being ferried back to the United States after several months of survey work in Japan. The contract called for approximately 1060 line miles of data acquisition, reduction and map compilation, mobilization and demobilization for approximately $40,000.

Survey Specifications and Statistics

The survey area included approximately 340 square miles (900 km^2) along the east rift zone, extending from Kilauea Volcano northeast to Cape Kumukahi. Elevations in the survey area vary from sea level to 3600 feet, with 60% of the area below 1000 feet. The survey crew arrived on site February 5 and began data acquisition on February 10 following equipment installation, calibration and compensation flights. Flying was completed on February 16.

The survey was flown as two adjacent blocks, A and B, as shown in Figure

3. Flight lines were flown N35°W at an average altitude of 500 feet (152 m) above mean terrain. The flight line spacing was approximately 1320 feet (400 m) in Block A and approximately 2640 feet (800 m) in Block B. Flight lines were extended approximately one mile beyond the coast line in order to help evaluate the presence of transverse structures and the average magnetization contrast along the ocean-island boundary. The navigation was visual with Doppler radar assistance. The flight path was recorded by a video recording system and later recovered from the magnetic tapes. Six tie lines were flown at N55°E along the trend of the rift to aid in discriminating between transverse structures and flight line leveling problems.

Instrumentation for the survey included a Geometrics airborne magnetometer with a sensitivity of 0.20 gamma, Doppler navigation system, radar altimeter and barometric altimeter. All data were recorded on digital magnetic tape and on an analog (strip chart) recorder. A base station magnetometer with a resolution of 0.25 gamma recorded the diurnal magnetic field variation and monitored the level of magnetic storm activity during all flying periods.

Data Compilation and Contractor Deliverables

Flightline position was recovered from the video camera tapes and a digital position grid was established for the compilation. The total magnetic intensity data were leveled using two of the six tie lines, and the 1980 International Geomagnetic Reference Field (IGRF) updated to 1983, was removed prior to plotting at a scale of 1:24,000. Paper preliminary plots of the contoured aeromagnetic data and profile plots were received from Geometrics on March 13 and 19 respectively. Corrections were made and annotations added to maps as requested, and the final mylar contour maps and profile plots were

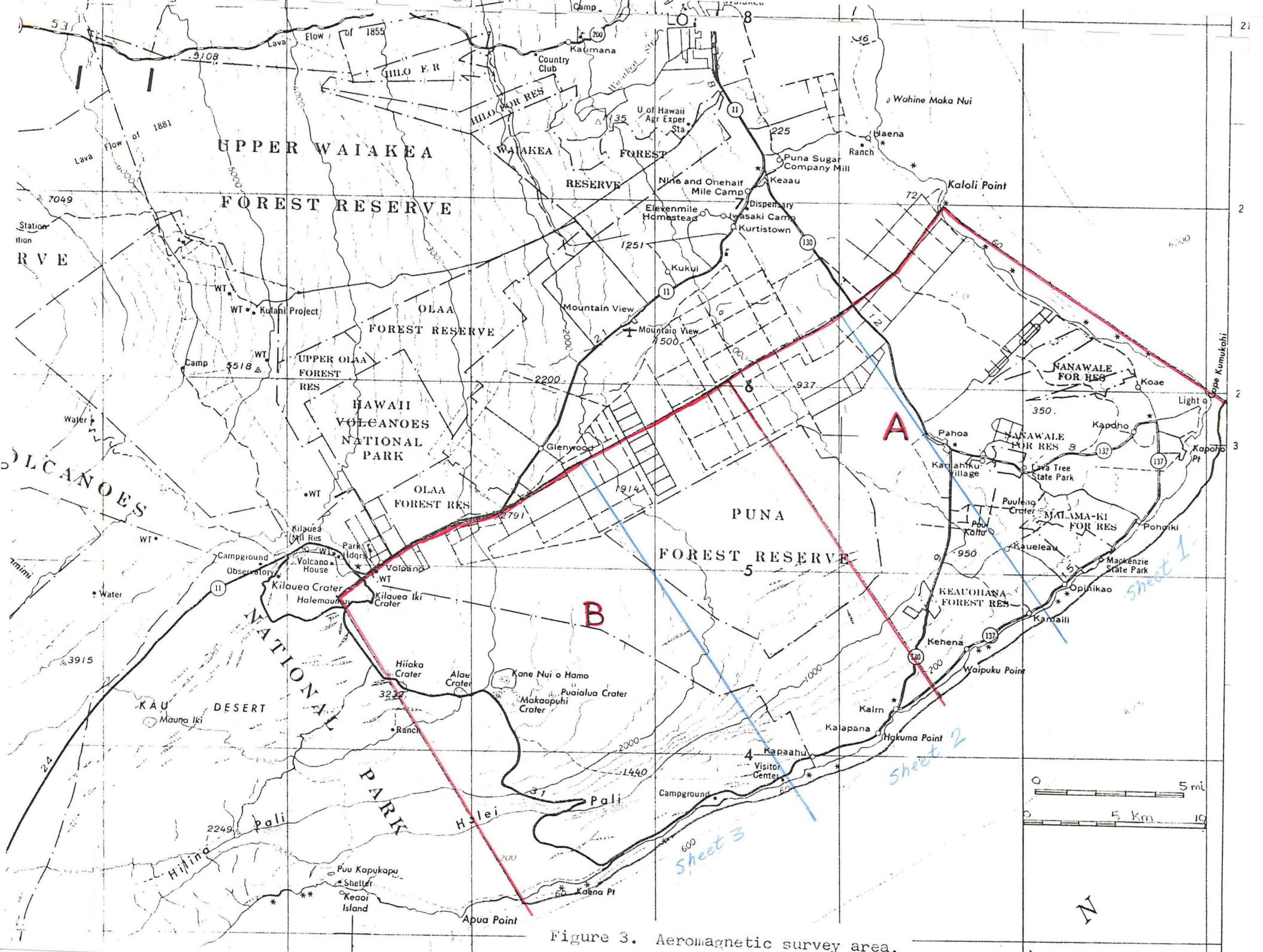

Figure 3. Aeromagnetic survey area.

shipped by Geometrics on April 1, 1983.

The deliverables received from Geometrics include:

1. Topographic maps at 1:24,000 with intended flight path and flight path recovery picks.
2. Video cassette tapes of the flight path.
3. Strip chart records of the ground magnetic monitor.
4. Observer's flight logs.
5. Strip chart in flight records of magnetic intensity, barometric and radar altimeter.
6. Located data tape and grid tape documentation.
7. Digital magnetic tapes, 9-track, 1600 BPI EBCDIC, for in flight data; located data tape; and grid tape of magnetic data.
8. Paper profile plots, horizontal distance scale 1:24,000, magnetic intensity scale 50 gammas/inch and 400 gammas/inch; also radar altimeter and barometric altimeter plots.
9. Mylar maps at a scale of 1:24,000 for: a) topographic base with flight path recovery and b) residual magnetic intensity.

This interpretation has focused on items 8 and 9 with only a cursory inspection of the back up data, namely items 1, 3 and 4. A few comments are in order for the final data items which have been studied in some detail and will be referred to in future interpretations.

Paper profile plots. These plots present the magnetic intensity, barometric and radar altimeter and terrain (barometric-radar altimeter values) for each flight profile at the map scale. Standard statistics (maximum, minimum, mean, and standard deviation) are printed for each parameter on the profile plot. The profile plots are of high quality and at appropriate scales for study and interpretation.

Magnetic contour maps and base maps. A map scale of 1:24,000 (identical to topographic base maps) was chosen for the compiled magnetic maps in order to retain as much position detail as possible throughout the interpretation. A map of the survey area at this scale is approximately 40 by 80 inches, too large for printing and convenient study. The data are therefore presented as three sheets approximately 40 by 30 inches in size, oriented along the northwest flight line direction, as indicated in Figure 3.

Contour intervals on the magnetic maps are 20 and 100 gammas, and magnetic lows are indicated by hatchures. The contour maps are of high quality and properly represent the profile data (not always the case in digital compilation procedures). The minor contour lines are too light and contour values too small for optimum presentation, but could not be improved without substantial added expense. Numerous closed lows were not hatchured by the contractor, but have been annotated during this study.

The Flight Path Recovery and Topographic Base Maps (set of 3 sheets at 1:24,000) and Residual Magnetic Intensity Maps (set of 3 sheets at 1:24,000) provided by Geometrics are not reprinted and distributed as part of this report because of the large size, level of detail and number. The original mylar maps have been transmitted to Thermal Power Co.-Geology where prints can be made and copies distributed as necessary. Future users should note that numerous closed lows were not hatchured by the contractor. These lows are annotated on a set of three 1:24,000 scale sepia mylar prints submitted as the detailed interpretation, file copy, to Thermal Power Co.

All deliverables (basic data) made available by Geometrics (itemized earlier) have been shipped to Thermal Power Co.-Geology for company archives. I recommend that all digital magnetic data tapes properly

identified and accompanied by format information be transferred to the Natomas data processing center for safekeeping.

The magnetic survey data are presented in this report as a single sheet composite map at a scale of 1:100,000 (Plate II). The scale is convenient to handle and overlies the generalized geology (Plate I) and data sets presented in an earlier report. Plate II is a direct 1:100,000 scale reduction of the original 1:24,000 scale maps and at a 1:4 reduction many contour values, hatchures and lines are illegible. A higher quality composite map would require recontouring from the digital grid tape at a scale of 1:50,000 or smaller with further reduction if necessary. The Geometrics' cost estimate to do this was in excess of $1,200 and was considered unnecessary at this time.

INTERPRETATION

Procedures

The initial phase of this interpretation required a detailed study of the profile plots to establish the validity of the final contoured map. The digital compilation accurately represents all the major anomalies recorded on the primary (NW-SE) profiles although short wavelength and low amplitude anomalies are better defined on the profiles. These anomalies generally arise from shallow depths and generally relate to topographic features or near surface lava flow features rather than major structures or deeper features of interest to Thermal Power Co. The magnetic profiles of the tie lines indicate some minor shifts of maxima, minima and gradients as compared to the contoured map. The tie lines are particularly useful in establishing the validity of transverse structures which may be confused with compilation effects. Inspection of the contour maps and tie line profiles indicates very little

contour elongation along flight lines, further indication of a high quality compilation. A review of the flight path recovery indicates very few location picks for flight lines in sheets 2 and 3, the western half of the survey. This is probably due to the vegetation density in the Puna Forest Preserve, the lack of identifiable topographic and cultural features, and smoke and haze resulting from the eruptive activity and resulting forest fires. Each profile has positive location points along a highway near the northwest border and along the seacoast. The relatively uniform topography and doppler assisted navigation probably guarantee a correct flight path but any substantial variation in aircraft speed would result in some small position errors along the profile. The net effect of these errors, if present, appears to be very minor.

Correlation of the radar altimeter and magnetic profiles indicates that reduced terrain clearance over well defined topography features, generally hills or craters, result in small (<100 gamma) anomalies. These do not significantly perturb the contour map at the 100 gamma level. Depth estimates based on the steepest linear gradient of individual anomalies on the profiles indicate that the great majority of all magnetic anomalies and trends arise from magnetic contrasts at shallow depth, typically 0-1000 feet. Deep magnetic sources appear to be relatively few, or are obscurred by the dominant effect of shallow sources, typically rift features or lava flows.

A detailed spatial correlation between mapped geology (Moore, 1982) and the residual magnetic intensity for the Pahoa South quadrangle further indicates that individual lava flows can give rise to anomalies or trends of 50 to 100 gammas, and infrequently over 100 gammas. The complex flow geometry indicated by Moore can be extrapolated throughout much of the survey area and

aid in understanding the multitude of lower amplitude features on the magnetic map. Correlation with Moore's (1981) map further establishes the south maximum-north-minimum-positive gradient expression common to the central rift zone throughout sheets 2 and 3.

Numerical modeling was used extensively to quantify the interpretation and to help determine the location of magnetic source bodies more accurately. An initial model set was computed to represent topographic features, thin flow like bodies, elongate bodies in the rift zone and transverse features to the rift zone. The models were calculated for the earth's magnetic field parameters of Hawaii, i.e. inclination = 37°; declination = 11°E, total field intensity = 37,500 gammas. These models helped to establish the source position and shape for most anomalies which were studied in the general sense.

Specific numerical models were computed for six anomalies important for a detailed understanding of the rift zone and the geothermal system. Each model required several (4 to 11) iterations to arrive at a satisfactory representation of the selected anomaly. All models were computed on the Earth Science Laboratory (ESL/UURI) PRIME 400 computer using programs GM3D and MREGON for three dimensional and 2 1/2 dimensional bodies, respectively. Model results are presented in Appendix I. Two characteristics of simple body anomalies at this field inclination are illustrated in Figure 4. The anomaly source body extends roughly from the anomaly maximum (on the south) to the polarization minimum on the north, with a strong gradient across the center of the body. The amplitude of the anomaly maxima and minima are approximately equal at this magnetic field inclination.

Table I summarizes the location and key characteristics of the anomalies

Table I. Numerical Models

NAME/AREA	DIMN.	MODEL DESCRIPTION	RESULT
Kapoho Crater	3-D 2 1/2-D	Large body of low susc. or reversed magnetism directly beneath Kapoho Crater apparent susc ∿ 0 μcgs d = 1500 ft.	High temperature or intrusive?
Kapoho State	3-D 2 1/2-D	Complex positive source with interior low susc body includes HGP-A, KS-1, KS-2	Complex structure above reservoir
Puu Kaliu Rift (L36-39)	2 1/2-D	Wide dikelike model of high apparent susceptibility (14,000) in central rift zone	Central rift zone magnetization and shape
Lae O Kahuna Coast (L-24-26)	2 1/2-D	Dike model of high apparent susc (K ≃ 13,000) along coastline	Coastal dike complex
South Coastline Area (L-41)	2 1/2-D	Dike model of high apparent susc (K ≃ 17,000) along coastline	Coastal dike complex
Napau Coastline (L-78)	2 1/2-D	Dike model of high apparent susc (K ≃ 17,000) along coastline	Coastal dike complex

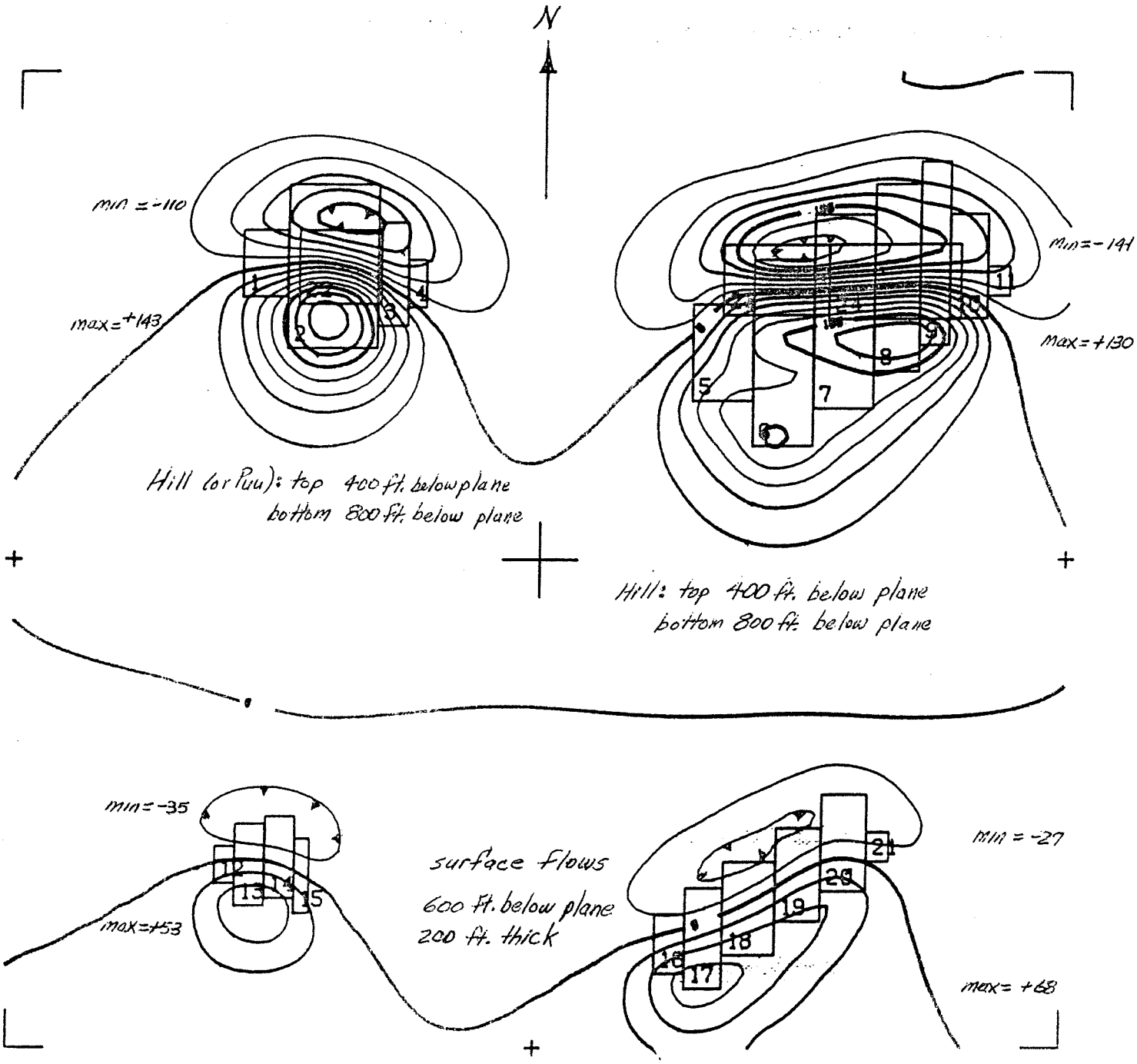

PROJECT NAME

TOPO & VENT AREAS

susceptibility (K) = 5000 μ cgs

MODEL NAME

MODEL 2

NUMBER OF PRISMS: 24.

MAGNETIC MODEL (GAMMAS)

GRID PARAMETERS

GRID POINTS X 29. : Y 27.

GRID SPACING : 500. FEET

GRID DIMENSIONS X 14000. : Y 13000. FEET

GRID OFFSET X: 0. Y: 0. FEET

SCALE 1: 24000.

DATA MAXIMUM: 143.

DATA MINIMUM: -141.

CONTOUR INTERVAL 100.

Figure 4a. Characteristic anomaly shapes at Hawaii magnetic field parameters. Topographic and surface features.

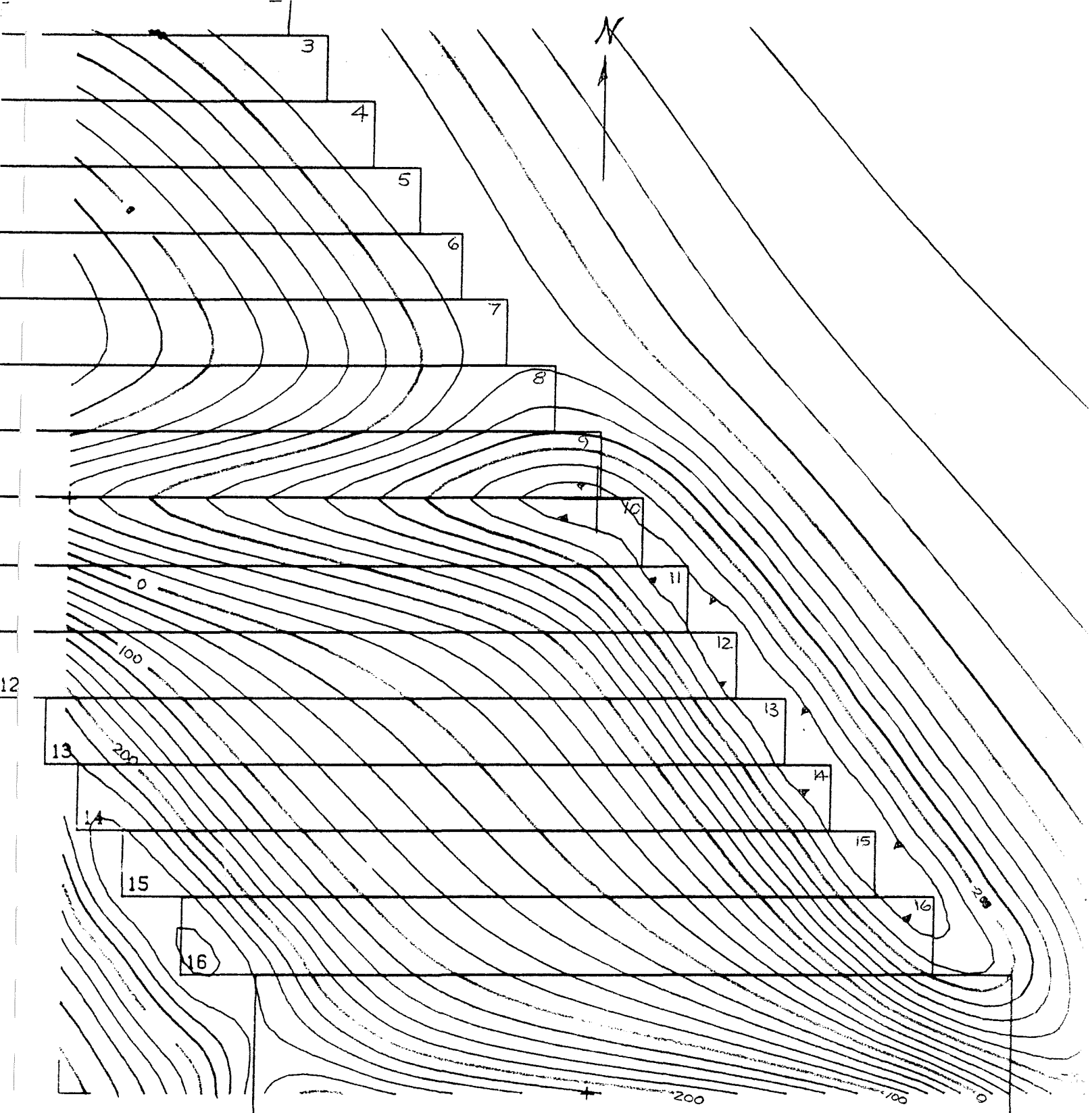

Figure 4b. Transverse structure.

PROJECT NAME

T-FAULT

Body 1-9: 2000 Ft. deep, 2000 Ft. thick

Body 10-17: 1000 Ft. deep, 2000 Ft. thick

MODEL NAME

K = 5000 μcgs

MODEL 1

NUMBER OF PRISMS: 17.

MAGNETIC MODEL (GAMMAS)

GRID PARAMETERS

GRID POINTS X 17. : Y 19.

GRID SPACING : 1000. FEET

GRID DIMENSIONS X 16000. : Y 18000. FEET

GRID OFFSET X: 0. Y: 0. FEET

SCALE 1: 24000. 0 1000 2000 Ft.

DATA MAXIMUM: 364.

DATA MINIMUM: -259.

CONTOUR INTERVAL 100.

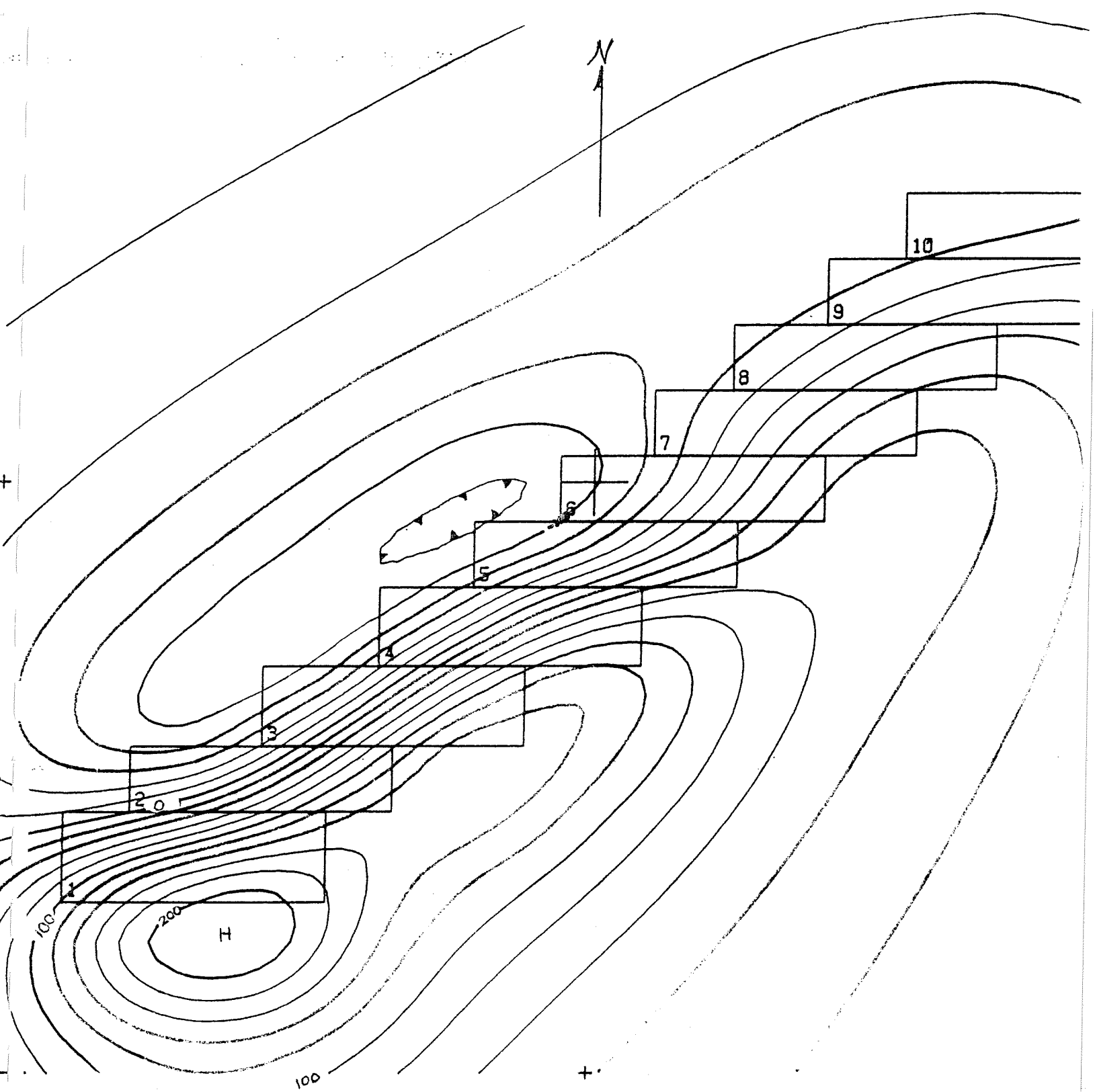

Figure 4c. Magnetic dike complex along rift.

PROJECT NAME

RIFT ZONE & DIKES

Body 1-5: 1500 Ft. deep, 4000 Ft. thick

Body 6-10; 2500 Ft. deep, 4000 Ft. thick

MODEL NAME

MODEL 3

K = 5000 μcgs

NUMBER OF PRISMS: 10.

MAGNETIC MODEL (GAMMAS)

GRID PARAMETERS

GRID POINTS X 18. Y 18.

GRID SPACING 1000. FEET

GRID DIMENSIONS X 18000. Y 18000. FEET

GRID OFFSET X: 0. Y: 0. FEET

SCALE 1:24000. 0 1000 2000 Ft.

DATA MAXIMUM: 218. 218

DATA MINIMUM: -122. -122

CONTOUR INTERVAL 100.

modeled in detail.

Interpretation Overview

The magnetic survey extends approximately one mile beyond the coastline on its northeast and southwest sides (Plate II). Steep negative gradients occur northwest of Cape Kumukahi and some closed lows are defined. This is consistent with the regional aeromagnetic survey (Godson et al., 1981) and results primarily from the magnetic land mass-to-sloping ocean bottom transition (the magnetic contrast being lava to sea water). The southeast sea coast is typified by low values offshore and low to high amplitude positive anomalies along the coastline.

Southeast Coast Rift Zone

The high amplitude anomalies are only partially indicated on the regional survey (Godson et al., 1981) because the mapped magnetic data terminate at the coastline. A low amplitude (50-200 gamma) positive anomaly along the coast is consistent with a sloping seafloor and island mass composed of low to moderate susceptibility (1000-5000 μcgs) lavas. The high-amplitude (600 gammas) closed highs on Plate II arise from dipping tabular bodies similar to the central rift zone. Figure 5 summarizes observed and computed magnetic anomalies for several models and two profiles perpendicular to the coastal magnetic anomaly. These model comparisons clearly show that a steeply dipping magnetic dike zone closely follows the coastline along the projection of the Hilina fault system (Plate III).

A limited review of periodic seismicity reports by the Hawaiian Volcano Observatory has indicated two recent periods of important seismicity along this coastal magnetic source. Figure 6 shows the epicenters of earthquakes of

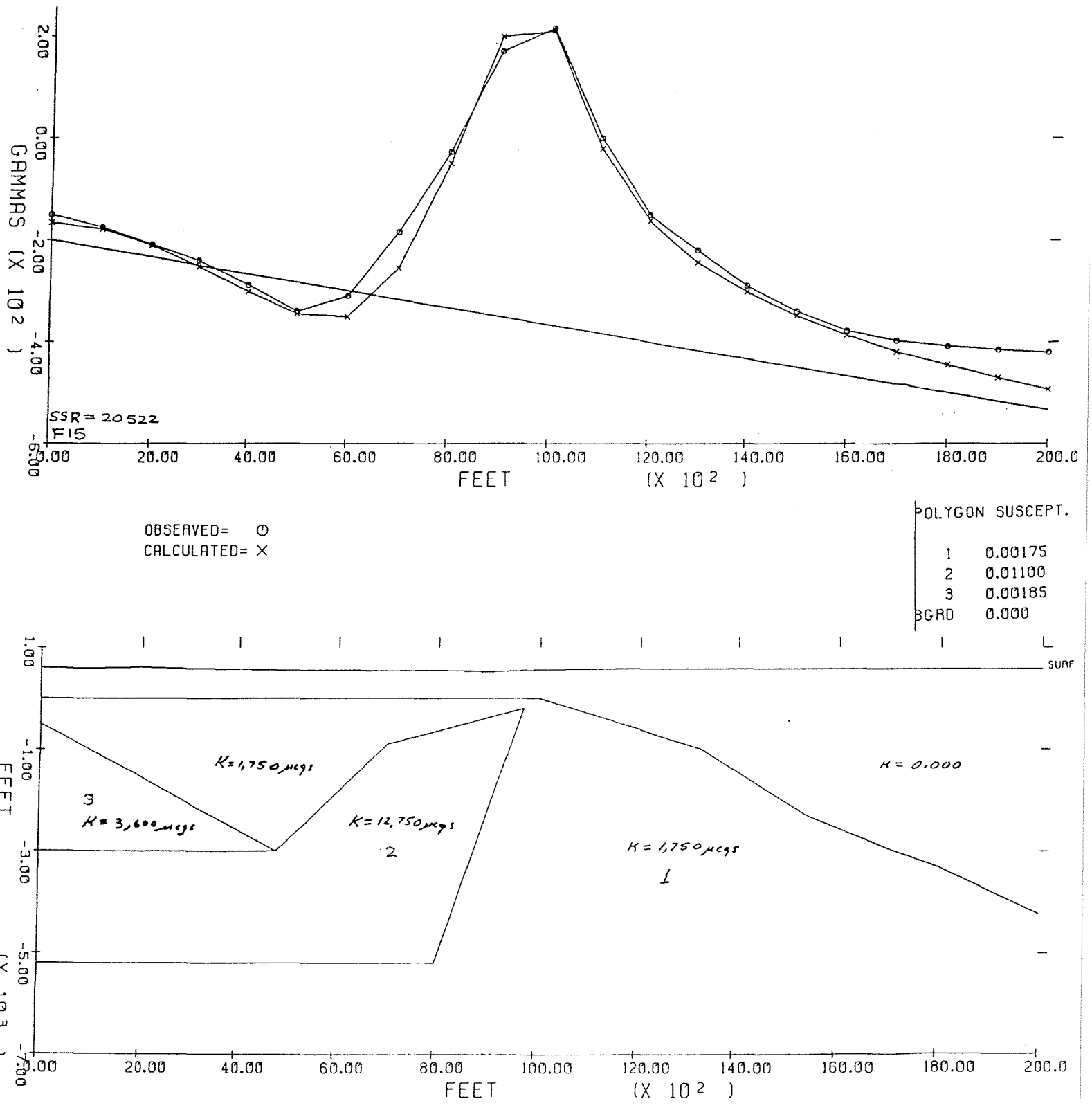

LAE O'KAHUNA COAST PROFILE #1

Figure 5a. Southeast coast model with dike zone.

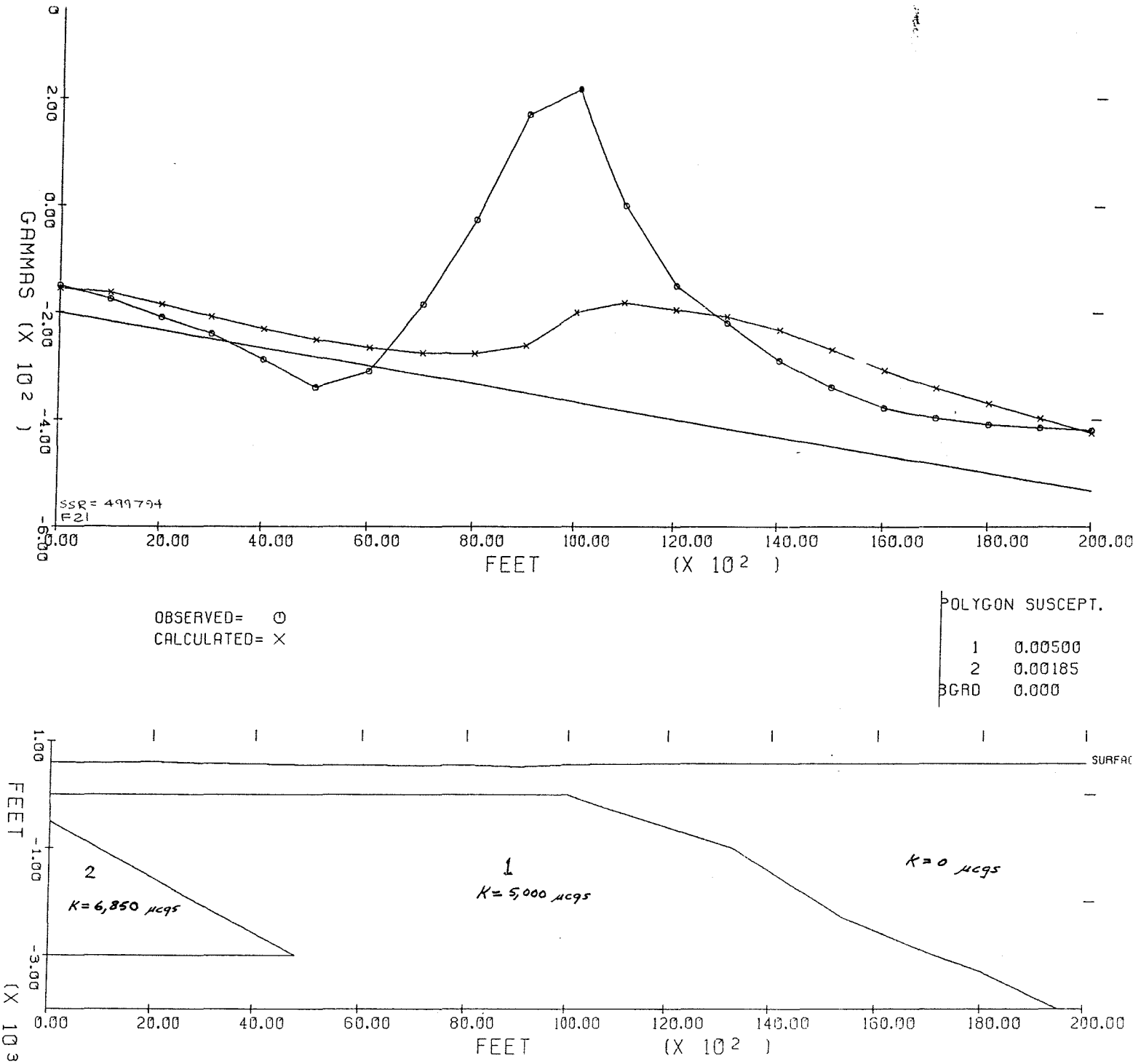

LAE O'KAHUNA COAST PROFILE #1

Figure 5b. Southeast coast model without dike zone.

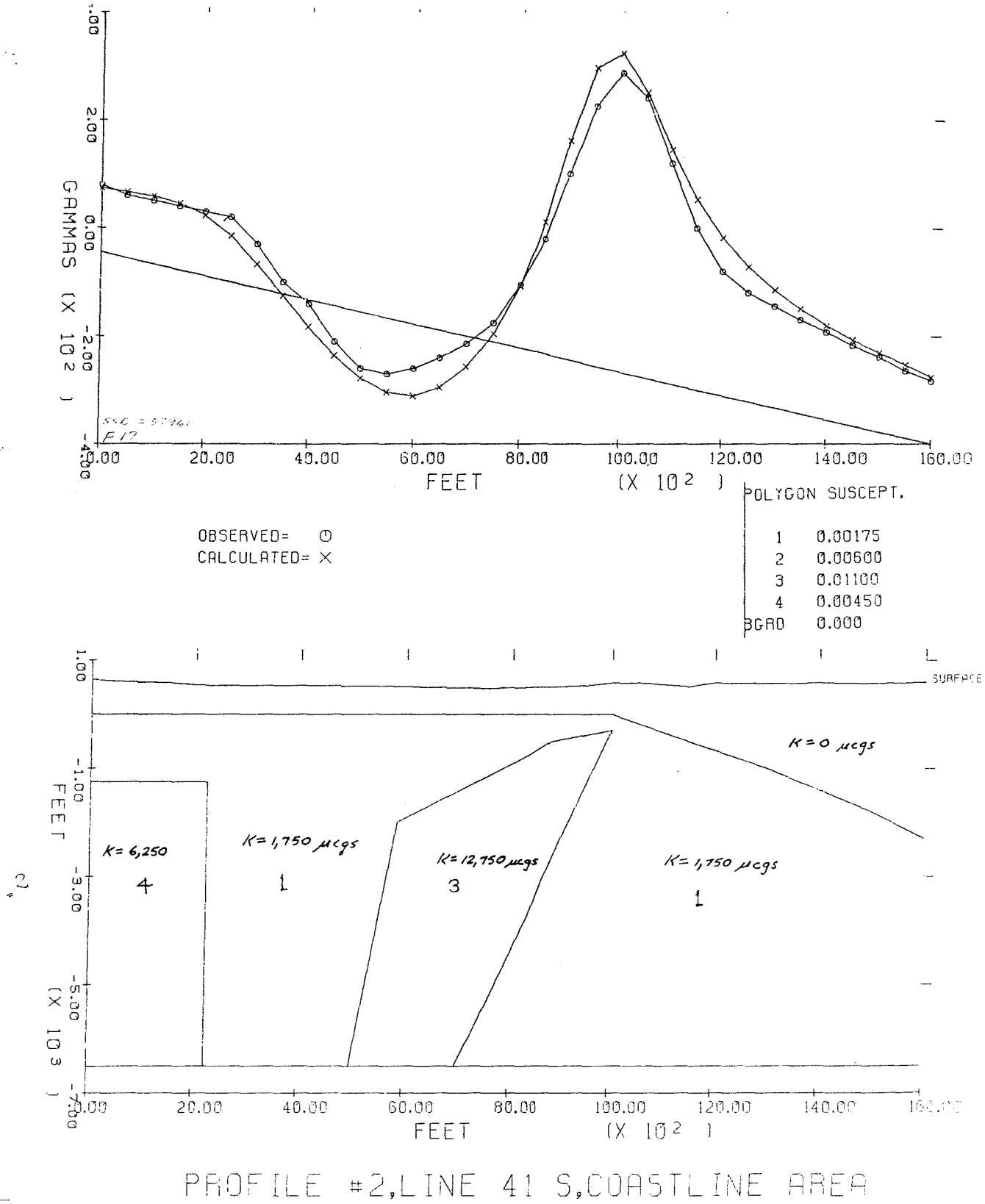

Figure 5c. Southeast coast model with dike zone.

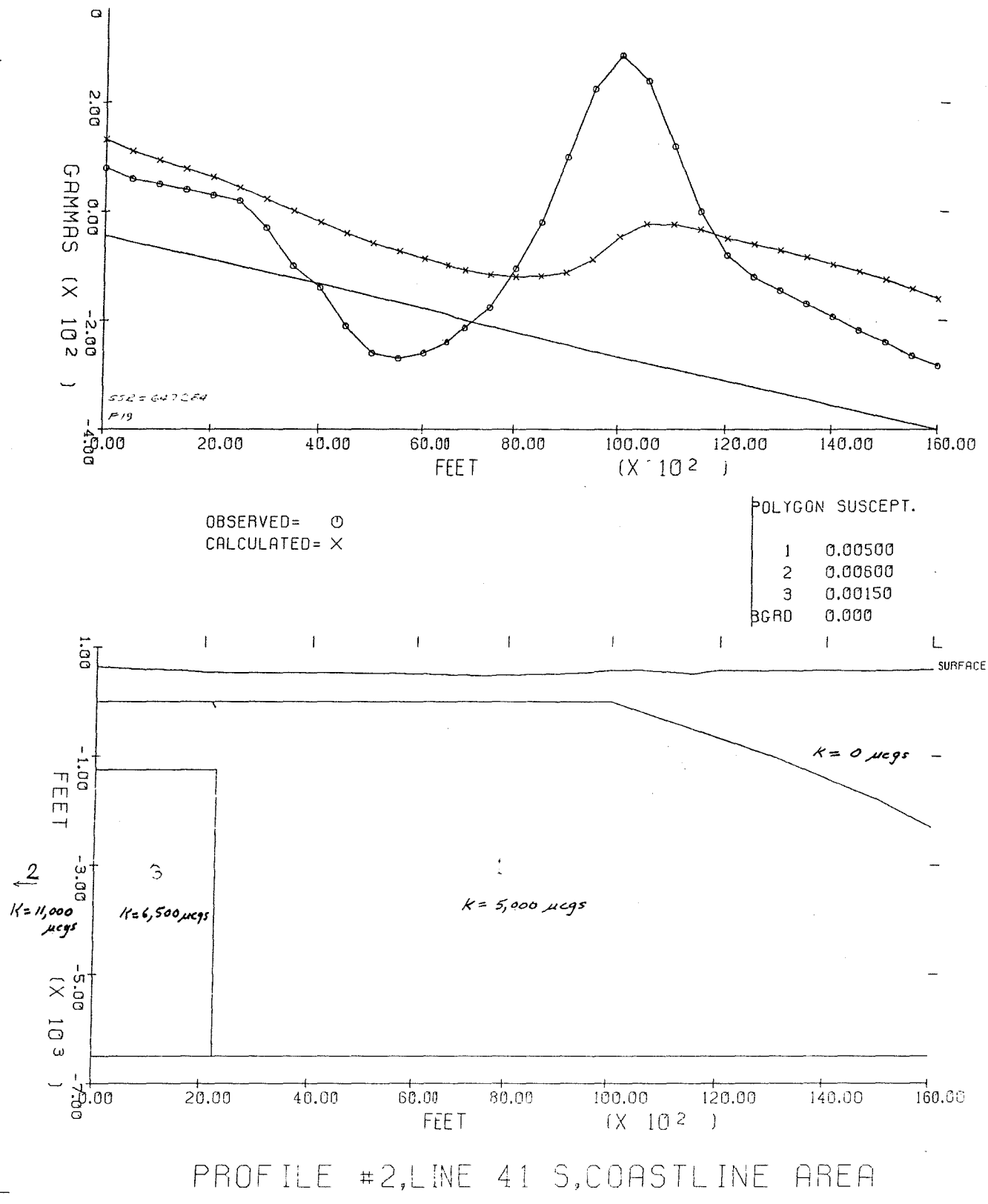

Figure 5d. Southeast coast model without dike zone.

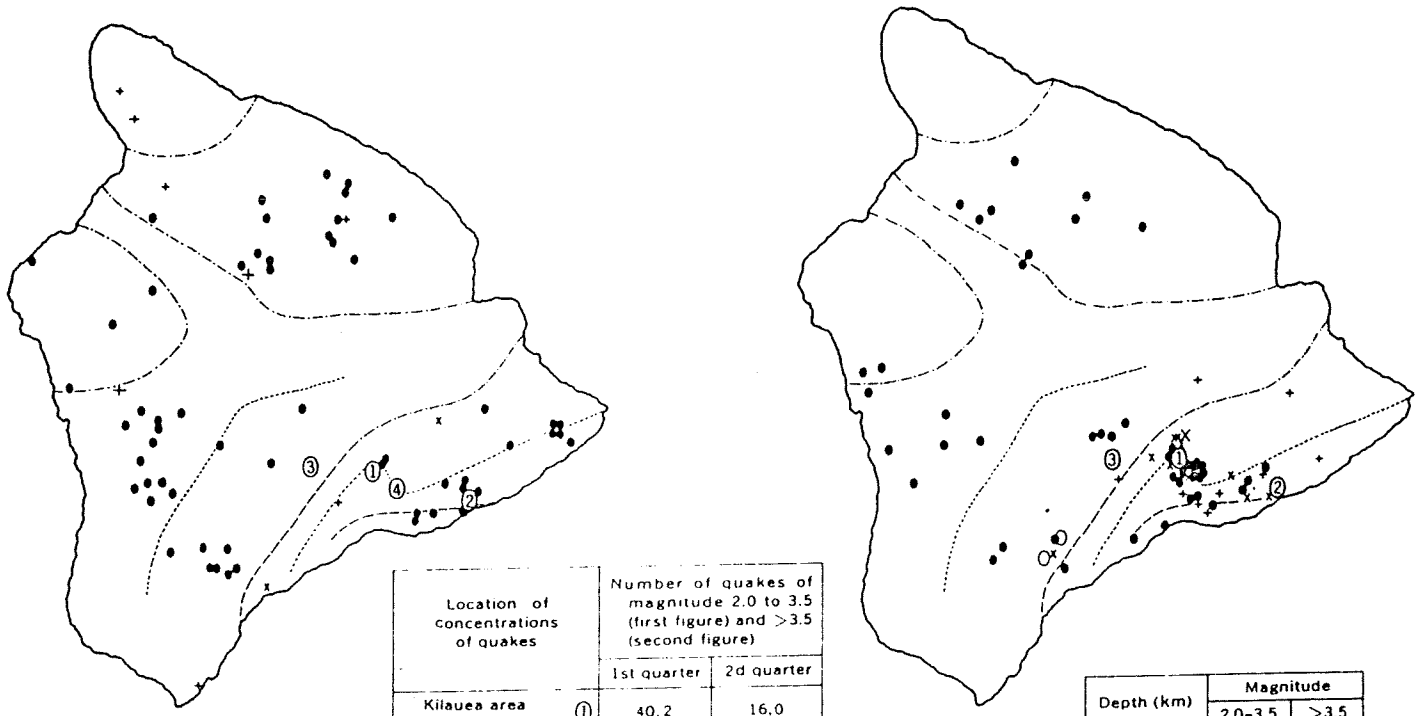

Location of concentrations of quakes	Number of quakes of magnitude 2.0 to 3.5 (first figure) and >3.5 (second figure)	
	1st quarter	2d quarter
Kilauea area (30-km depth) ①	40, 2	16, 0
Kalapana Trail area ②	4, 0	2, 0
Kaoiki fault system ③	11, 0	22, 1
Upper east rift zone ④	8, 0	?, ?

Depth (km)	Magnitude	
	2.0–3.5	>3.5
<10	•	O
10–20	+	+
20–60	x	X

FIGURE 6a.—Epicenters of earthquakes of magnitude 2.0 and greater for the first quarter (*left*) and second (*right*) of 1963. The number symbols identify concentrations of quakes that are listed in the left-hand table because they are too numerous to plot separately, and represent the following areas: (*1*) Kilauea, at a depth of 30 km; (*2*) along the Kalapana Trail, which extends south of Kilauea's east rift; (*3*) along the Kaoiki fault system; and (*4*) along the upper east rift zone of Kilauea. Geographic names are shown on figure 1. The number of earthquakes in the upper east rift and including the adjacent Koae fault system was difficult to determine accurately during the May 9–12, July 1–5, and August 3–5 seismic crises, and the August 21–23 Kilauea east rift eruption because of the complexity of the seismograms.

(from Koyanagi and Endo, 1965)

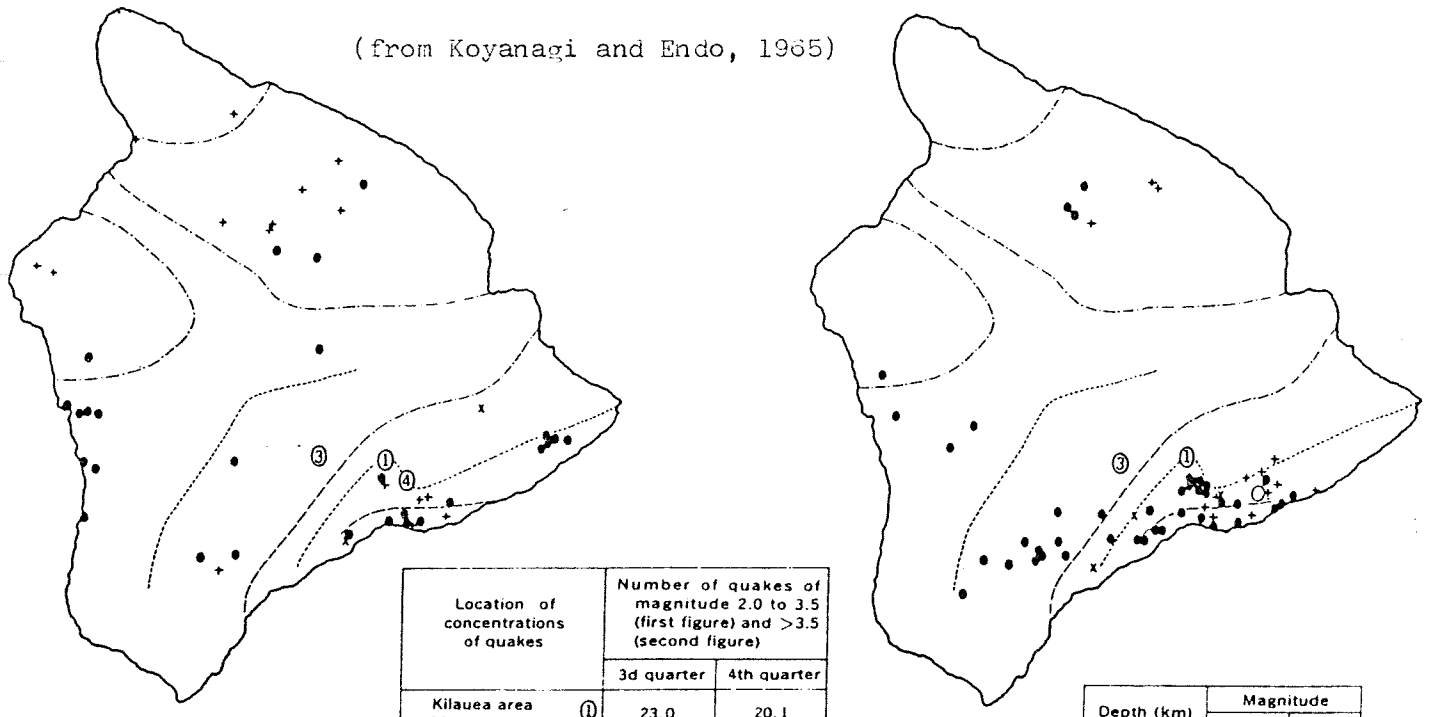

Location of concentrations of quakes	Number of quakes of magnitude 2.0 to 3.5 (first figure) and >3.5 (second figure)	
	3d quarter	4th quarter
Kilauea area (30-km depth) ①	23, 0	20, 1
Kaoiki fault system ③	44, 3	44, 3
Upper east rift zone ④	82 ±, ?	?, ?

Depth (km)	Magnitude	
	2.0–3.5	>3.5
<10	•	O
10–20	+	+
20–60	x	X

FIGURE 6b.—Epicenters of earthquakes of magnitude 2.0 and greater for the third quarter (*left*) and fourth quarter (*right*) of 1963. The number symbols identify concentrations of quakes that are listed in the left-hand table because they are too numerous to plot separately, and represent the following areas: (*1*) Kilauea, at a depth of 30 km; (*3*) along the Kaoiki fault system; and (*4*) along the upper east rift of Kilauea. No quakes of this magnitude were reported for the Kalapana Trail area (location 2, fig. 2). Geographic names are shown on figure 1. The number of earthquakes in the upper east rift during the October eruption on the east rift of Kilauea was difficult to determine accurately because of

FIGURE 7.—Quarterly plot of epicenters of earthquakes of magnitude 2.0 or greater beneath the island of Hawaii during 1965. Dot-and-dash lines are boundaries of volcanic systems, long-dashed lines are fault systems, and short-dashed lines are rift zones. Geographic names are shown in figure 1.

(from Koyanagi, 1968)

magnitude 2.0 and greater for 1963 (Koyanagi and Endo, 1965). Figure 7 illustrates the seismic activity along the coast in 1965 (Koyanagi, 1968). During these periods the earthquake activity along the central portion of the rift was somewhat less than generally observed. Note also from Figures 6 and 7 the limited number of epicenters located in the Pahoa-Cape Kumukahi area. This suggests a decoupling of tectonic activity, possibly along transverse structures identified in this study, from the main portion of the east rift zone.

East Rift Zone, Central Magnetic Anomaly

A large amplitude (500-1500 gamma) magnetic anomaly trends southeast from Kilauea Crater for 10 km then abruptly bends east-northeast for an additional 30 km along the southeast margin of the active rift zone (Plates II, III). The long sinuous anomaly varies in amplitude and appears to be offset in many places. The near surface projection of this shallow (500-1500 ft. deep) source is indicated on Plates III and VII. Numerical model results (Fig. 8) indicate a very high apparent susceptibility (10,000-16,000 μcgs) for much of this anomaly. Remanent magnetism inclined along the direction of the earth's field may contribute to the high susceptibility estimate. The rift magnetic anomaly terminates west of Kahuwai Crater, approximately one mile west of HGP-A (Plate VII).

Puna Geothermal System

A smaller (500 γ ; 1 mile diameter) isolated magnetic anomaly occurs over the Puna geothermal system, Plate II. Because of its association with the target area and some potential for delineating reservoir controls this anomaly has been modeled in some detail. The geometry of the magnetic sources is shown on Plates III and VII, and in numerical models, Appendix I. The main

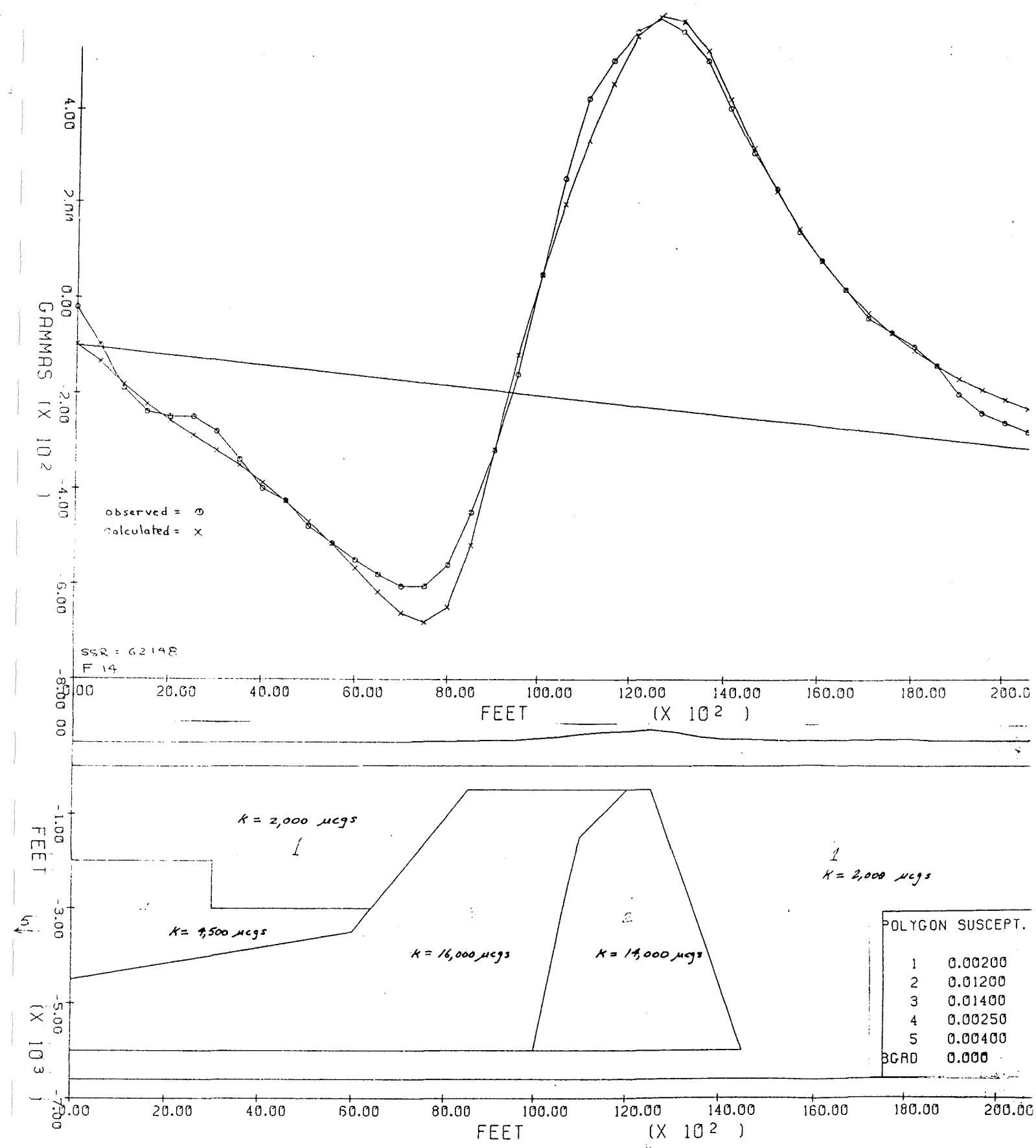

PUU KALIU RIFT, L36-L39, PROFILE #3

Figure 8. Puu Kaliu magnetic model and numerical model. (Central rift zone)

characteristics of the anomaly can be generated by a semi-circular shaped source almost 10,000 feet long along the rift and 5000 feet transverse to the rift in plan. The source occurs at shallow depths, 200-500 feet, and extends to depths of 3000 to 4000 feet - the bottom of the source is not well resolved. A relatively non-magnetic hole, perhaps 1000 by 3000 feet in plan dimensions, occurs near the center of the source. Magnetizations typical of lava flows occur to the north and typical of the dike complex occur to the south and west. Weakly magnetic rocks appear to surround the source (Plates III, VII). The HGP-A, KS-1 and KS-2 drill holes would appear to be drilled through the magnetic source into less magnetic rocks at depth.

Kapoho Crater Anomaly

Another significant magnetic source is located three miles downrift from the Kapoho geothermal wells. A sharp magnetic low (990 γ below background, Plate II) occurs south of Kapoho Crater and a broader magnetic high (750 γ above background) is symmetrically located north of the crater. This is the reverse of the anomaly disposition about a positive magnetic source in the northern hemisphere and implies either: 1) reversed remanent magnetism or 2) very low susceptibility and remanence as compared to surrounding rock. The last major magnetic field reversal is dated at approximately 700,000 years (Mankinen and Dalrymple, 1979), much older than the Kapoho Crater source. The source appears to be a large area of near zero magnetization caused by one of the following: an intrusive body with much less magnetite than surrounding lava or dikes; a large well defined area of extensive alteration and nearly complete magnetite destruction; an area of above Curie Point ($\sim$ 570°C) temperature. Some combination of the latter two possibilities seems most likely but the shallow source depth, 1000 feet, and lack of surface manifestations and high surface temperature argue against above Curie Point

temperatures as the main explanation. This anomaly is the most well defined area of low magnetization and hence possible zone of above Curie Point temperatures or extensive hydrothermal alteration in the entire survey. One other possible explanation would be an intrusive body with abnormally high titanium content. Low magnetic susceptibility results when titanium substitutes for some of the iron in the magnetite crystal lattice. This explanation seems unlikely.

Napau Crater - Puaialua Crater Anomaly

The wide, high amplitude rift anomaly is significantly reduced in width and amplitude, and develops a closed south side low south of Napau Crater, Plate II. The survey was flown early in the current eruptive phase, which began at Napau Crater. The area of reduced magnetization could well result from a sizeable body of magma, or large volume of rock above the Curie Point temperature, at shallow depth. Several other distinct magnetic lows on Plates II and III (Iiewa Crater, Kilauea Iki, and Makaopuhi Crater) also suggest very low magnetization (high temperatures). No numerical modeling has been undertaken to quantify an interpretation for this area because further proof of high temperatures may not be of great exploration value for these areas.

Transverse Trends and Structures

In an earlier study Ross, (1982) noted trends in regional aeromagnetic, self-potential, seismic and gravity data which were oriented transverse to the rift. The detailed magnetic data and the composite magnetic map, Plate II, indicate the presence of such structures as northwest trending gradients, specific low amplitude anomalies, and more convincingly, as offsets in or disruptions to the seacoast and central rift anomalies. These northwest trends lie parallel to the flight path direction and may occasionally be

enhanced by differences in survey altitude or position errors along the flight path. Examination of the six tie lines supports the interpretation of transverse structures indicated in the interpretation, Plates III and VII.

Other Anomalies

As noted earlier numerous low amplitude anomalies and trends are present on Plate II. Many of these can be attributed to specific flows or topographic features. Numerous other anomalies, north of the active rift zone have not been interpreted in detail because they probably have little relationship to the geothermal exploration program. Numerical modeling could establish basic geometries and magnetizations of these features, should this be desired at a later time.

SUPPLEMENTAL GEOPHYSICAL DATA

General Data Base

Ross (1982) reviewed a broad spectrum of geophysical data for the Kilauea east rift zone and compiled a series of basic data plates for regional magnetic, gravity, seismic, self-potential, bipole-dipole (reconaissance) electrical resistivity and detailed electrical resistivity data. Observations on these data are not restated here but significant new observations resulting from an integration of the detailed magnetic data or the ARCO geophysical surveys are noted in a later chapter, Discussion.

This is an appropriate place to comment on differences between the detailed magnetic data of Plate II and the regional aeromagnetic data of Godson et al. (1981) presented as Plate III in Ross (1982). The increased detail of the 1983 Geometrics survey results from several factors: reduced flight line separation (0.25 or 0.50 mile vs. 1.0 mile); reduced terrain

clearance (550 feet vs 750 feet); flight lines perpendicular to major trends (i.e. N35°W rather than north); data reporting scale (1:24,000 vs 1:250,000); and extension of flight lines for one mile beyond the coastline. Numerous differences in anomaly amplitude, shape and complexity are present as may be expected. The coast line dike complex anomalies are suggested locally by the regional data, but not well defined. The main rift anomaly is similar, but is located one mile too far to the north on the regional map. The geothermal area appears as background level or a very weak high in contrast to the well defined one-mile diameter anomaly on the detailed data. The Kapoho Crater anomaly appears as a positive source north of the crater rather than a low susceptibility zone beneath the crater.

Most important for our structural studies is the difference between north-south transverse trends on Godson et al. (1981) and the northwest trending discontinuities and trends seen in the detailed data. Flight line/compilation effects in the regional data are the main cause for this discrepancy. Four of the transverse structures noted earlier (Ross, 1982, Plate VIII) are verified by the new data where they cut across the strong rift anomaly; the trend of the structures however is different. Accordingly, the 1982 structural interpretation based on regional magnetic data (Plate VIII) is superseded by Plates III and VII of this report.

ARCO Self-Potential Survey (MicroGeophysics Corporation)

The self-potential (SP) survey was completed from April 5 to May 22, 1978 by a two man crew using standard state-of-the-art equipment and a 100 meter sample interval. The survey included eight closed loops of several kilometers each, but the loops are not tied together or referenced to a common background voltage level. The contractor notes that some loops in the Puna Forest

Reserve required up to five days to complete due to the dense jungle and hazardous surface conditions. The linear distribution of drift (typically 1 to 11 mv per 100 m) must be considered subject to considerable error for these loops, although it is the only reasonable way to apply the corrections. This limitation does not substantially detract from the survey results since numerous anomalies exceeding 500 mv were recorded. The self-potential data, uncorrected for elevation, are presented at a scale of 1:100,000 as Plate IV.

The self-potential surveys in the Puna area generally substantiate the results of Zablocki (1977) but are based on fewer profiles and thus have less spatial resolution. Microgeophysics has extended the Nanawale Estates anomaly (Zablocki's anomaly D) and concludes that the anomaly is probably not cultural as dismissed by Zablocki. The anomaly remains open to the west.

A weak SP high or ridge extends along the road above Pohoiki, cutting across the negative anomaly typically noted along the south side of the east rift. This observation provides additional support for a cross cutting structure in this area, as proposed by Zablocki (1977).

The principal contribution of the self-potential survey is the several loops which cross the Puna Forest Reserve, the southwest rift area, and north of Kilauea. These are totally new data which allow us to generalize the negative-positive-negative anomaly response as the central portion of the rift is traversed. None of these anomalies show an elongation perpendicular to the rift as pronounced as anomaly C near HGP-A, so they are presumably less favorable. The self-potential coverage across the rift remains incomplete, however. MicroGeophysics notes the SP high ridge follows the rift almost exactly except near Puu Kauka where the maxima is associated with active venting of steam. They feel the highs are generated by "hot water convecting

up along central and northern fault planes." Thus the SP appears to be a rather direct indicator of geothermal potential. Self potential lows are attributed to the movement of surface waters downward to the water table.

One shortcoming of the contractor's report, when one wishes to study it in detail, is the lack of tabulated data which would indicate in more detail the voltage difference between stations, total drift corrections, drift between reoccupations of a base station, and time between readings. Additional study might justify a more exact elevation correction instead of the uniform 1.8 mv per m above sea level routinely applied to all the data. This may be an alternate explanation for SP contours which do not parallel the coast line south of HGP-A.

ARCO Microearthquake Survey (MicroGeophysics Corporation)

The microearthquake survey was conducted from April 5 to May 22, 1978, concurrent with the self-potential survey, for a total of 48 days. Six to 10 microearthquake recording stations were operational on any one day and a total of 75 stations were occupied. In this manner the roving seismic array was modified at a rate of 2 or 3 stations per day, and a given station was occupied for 3 or 4 days. The result was an excellent survey which covered a large area with a fairly uniform distribution of stations. The effective recording time for a given area was held fairly constant at 4 to 7 days. Thus the contractor has achieved as good a map of seismicity distribution with time as one could expect while working in a short term exploration mode. The detection limit was typically 0.0M or 1.0M events with the higher detection limit resulting from more widely separated stations in the less accessible areas, i.e. the Puna Forest Reserve, and wind noise transmitted to the earth by means of the dense vegetation.

Microgeophysics detected a large number of events and was able to locate 378 hypocenters. The high background noise levels and number of active structures precluded studies of surface velocity structure and fault plane solutions.

The hypocenter locations presented in map and section form contain a great amount of geologic information. Plate V presents the hypocenter locations at the regional data base scale (1:100,000). Some of the more important features are:

- Eight hypocenters located within a 4 sq km area centered about HGP-A (colocated with low resistivity anomaly AR of Plate VIII, Ross, 1982).

- 10 or more hypocenters may be colocated with the poorly defined low resistivity area DR (Plate VIII, Ross, 1982). A few hypocenters occur in the positive SP anomaly A of Plate VIII, Ross, 1982.

- Few, if any, hypocenters were located in the other low resistivity zones (GR, CR, ER, FR) identified in an earlier report. Only two hypocenters were located east of the northwest trending alignment which crosses the geothermal area suggesting that the eastern tip of the island may be decoupled from the seismicity to the west along this structural zone.

- A high density of hypocenters for more than 100 events occurs along the sinuous magnetic anomaly in the Chain of Craters area.

- Six northwest trending alignments of hypocenters which cut across the Chain of Craters. These indicate the presence of cross cutting structures.

- Numerous hypocenters appear to be "offset" to the south of the rift in the area from five to 11 km west-southwest of HGP-A.

- There is some correlation between hypocenter locations and magnetic source bodies identified earlier; in addition some magnetic source areas are devoid of events.

- The hypocenter locations agree well with the historic seismicity record for events $M \geq 2.5$ between the Pahoa - Kaimu road and Cape Kumukahi.

- These data present a totally new base of about 200 events west of Pahoa along the rift zone.

The microearthquake data provide considerable support for geologic structures and encouragement for increased permeability (and possibly magmatic or geothermal activity) in several areas. They represent an important data set for developing a more complete understanding of the east rift zone.

ARCO Time Domain Electromagnetic Survey (Argonaut Enterprises)

Argonaut personnel initiated their electrical studies with the preparation of electrodes for a 3500 foot long line source. An entire crew day was required to emplace steel stakes, sheet metal, brine solution and to haul in topsoil for the electrodes, and this effort resulted in a maximum 1 amp current input. As a result all further resistivity data were obtained using the large loop (2500 feet on a side) time domain electromagnetic technique, which does not require electrode preparation. The high resistivity first layer rocks are essentially transparent to the electromagnetic (EM) signal and are not resolved by the method.

The TDEM sounding plots, Volume 2 of the Argonaut report, were reviewed only briefly. The data are carefully presented and the depth/resistivity interpretations appear to be consistent with each other. Robert Furgerson is far more expert in interpreting loop-loop data than this author and a set of master curves would be necessary for a reinterpretation--few sets are available. The Argonaut TDEM interpretation should be accepted as presented.

The TDEM survey which Argonaut completed for ARCO covered a large area, including the southwest rift zone northeast to Cape Kumukahi, so it is necessary to evaluate the data coverage throughout the area. This can be

summarized as below:

Area	Source Loops	Receiver Stations	Coverage
Puulena Crater-Cape Kumukahi	4	50+	Good; detailed
Kalapana-Pahoa	2	33+	Fair; reconnaissance
Kilauea SW Rift	3	45	Good; reconnaissance
Kilauea NW Rift	2	26	Fair; reconnaissance

There is a data gap of approximately 12 miles along the rift in the Chain of Craters area.

A total of 169 soundings were completed about 11 source loops. The quality and interpretation content is summarized below (Argonaut Enterprises, 1978):

Total Soundings		169
-Weak signal or too noisy	33	
-Transients with negative onsets (complex geometry)	15	
-Soundings suitable for interpretation	121	
• Homogeneous earth solutions	79	
• Two layer earth solutions	42	

The TDEM survey adds about 20 new sounding solutions in an 8 by 8 km area around the Puna geothermal system, and thus provides better control on the general resistivity structure than the HIG EM studies. Keller's bipole-dipole work had many more Tx - Rc legs in the area however, and probably offers better lateral (though poorer vertical) resolution of the resistivity distribution. The large Tx - Rc separations required for the loop-loop method (3-7 km as used here) necessarily limit the amount of detail and spatial resolution. Plate VI integrates the eastern portion of the Argonaut survey with earlier TDEM data, at a scale appropriate for detailed exploration evaluation.

The important observations noted from a correlation of Argonaut's interpretational plates and our 1:100,000 data base are:

- The northwest trending structural zone infered from TDEM data includes most of the structural zone interpreted from gravity, magnetic, and seismic data (Ross, 1982). Argonaut's zone is twice as wide and trends N45°W as compared to the N10°W zone interpreted earlier.

- The KS, HGP-A wells occur in a slightly higher resistivity "saddle" as contoured by the TDEM best conductor and TDEM deepest unit data. Resistivities at depth are 6 to 7 ohm-m compared to 3 to 5 ohm-m to the north and south.

- The resistivity patterns are in general agreement with the HIG data shown on our Plate V, but the lowest Argonaut values are 3-5 ohm-m versus 1.9 and 1.8 ohm-m of Kauahikaua and Klein's final interpretation.

- TDEM work does not delineate the high resistivity zone of K and K Tx 1 for reasons noted earlier, i.e. a "transparent high resistivity upper layer".

- An anomalous low resistivity zone occurs approximately 2 1/2 miles (4 km) southwest of Pahoa; it is open to the northwest.

- Three very anomalous stations occur in an area centered 5 miles (8 km) northwest of Kalapana on the edge of the Puna Forest Reserve. The sounding plots suggest the data are strongly effected by a nearby lateral change in resistivity (Argonaut Enterprises, 1978).

- Three other areas of anomalous low resistivity occur west of the Puna Forest Reserve, near Kilauea Crater.

- There are no soundings in the Puna Forest Reserve due to the dense jungle and dangerous terrain.

Integrated with earlier TDEM studies (Keller et al., 1977) and bipole-dipole resistivity results, an improved map of geoelectric structure can be produced for the Puna area. Our interpretative map of resistivity structure based on all these data is presented as Plate VI. The geothermal reservoir borders cannot be delineated within ± 2000 feet with confidence from these data, however.

DISCUSSION

The detailed aeromagnetic survey provides a uniform high resolution data base which reflects the magnetization of geologic units for the entire east

rift zone. Because most of the lava flows and dikes which make up the east rift are quite magnetic, the magnetic field is dominated by variations in the upper 4000 feet of the subsurface. A detailed interpretation of deeper features would require sophisticated processing such as selective low pass filtering and removal of regional gradients, followed by more numerical modeling. I personally believe that little new detail for the sub 4000 foot structure would result from such an interpretative effort. The interpretation to date has identifed numerous subsurface features throughout the survey area, many of which are supported by geologic mapping such as surface faulting and fissures. Microearthquake hypocenters (MicroGeophysics, 1978) align along several interpreted transverse structures giving credence to the magnetic interpretation and further indicating which structures were active at the time of the seismic survey.

Several local areas of very low (approaching zero) magnetization have been identified within the normally very magnetic rift zone. Although only one anomaly, associated with Kapoho Crater, has been interpreted in detail, the association with magma at Kilauea Iki and Napau Crater suggest above Curie Point temperatures within 1000 feet of the surface may explain the magnetic low features. Similar anomalies occur at Makaopuhi Crater, southeast of Heiheiahulu Crater, at Lilewa Crater and Kapoho Crater. Detailed numerical modeling was not undertaken for sources other than Kapoho Crater because further information about these sources did not appear to have a great exploration value. Thermal manifestations such as recent flows and steaming fissures, and self potential highs suggest high subsurface temperatures in many areas along the rift zone. The geothermal potential however is probably limited by the hydrology and thus the detailed geometry of the dike complex at any given site. One would expect the upgradient side of the magnetic source

associated with the dike complex as a more favorable area for geothermal potential. Permeability within the rift may be locally enhanced along the interpreted transverse structures, especially those indicated as active by the microearthquake data, Plate V.

Puulena Crater-Cape Kumukahi Area

An extensive geophysical data base has been established for the eastern portion of the rift zone which includes the known geothermal resource between Puulena Crater and Puu Honuaula. These data sets must be integrated and weighed one against the other in an attempt to define the limits of the geothermal system. Plate VII attempts to bring the key data and conclusions together. Plate VIII presents the key physical property data and geometries in cross section.

A northwest trending structure, best defined in the magnetic data, cuts across the rift and terminates the 20 mile long magnetic anomaly which trends northeast from Kilauea Crater. A complex magnetic source which need not extend to great depth overlies the geothermal system (Plate VII), and may have been part of rift magnetic anomaly, now displaced to the north. Microearthquake activity, Zablocki's (1977) self-potential anomaly, and low resistivity zones at depth extend east of this structure. This structure logically bounds the known geothermal system on the west, although substanial permeability may be present immediately west of the structure.

An eastern limit to the geothermal system is not well defined. A second transverse feature corresponds approximately with an increase in resistivity at depth (1800-3000 feet). The distribution of transmitter loops and receiver stations is such that this resistivity border is uncertain to within a mile. Compounding the uncertainty are these observations: low electrical resistivity

(2-4 ohm-m) overlying deeper resistivity units as far east as Kapoho Crater; positive self-potential anomalies (Plate IV) continue east to Kapoho Crater, although poorly defined by the traverse lines and apparently of lower magnitude. In addition a large body of near zero magnetization underlies Kapoho Crater, perhaps only 1000 feet deep (Plates III, VII). There is some possibility that this is a cooling magma or intrusive body, and possibly part of the heat source for the thermal system. The low susceptibility area appears to be aseismic on the historical record and the microearthquake survey, Plate V. The resistivity data provide the best indication of a cutoff to the geothermal system at depth, the change from resistive over conductive to conductive over resistive structure, as mapped by Argonaut Enterprises (1978).

A zone of low electrical resistivity (2-5 ohm-m) extends both north and south of the productive wells without clear cutoffs in the geophysical data. The self-potential anomalies offer encouragement for near surface circulation in the Puulena Crater-Puu Honuaula area, and indicate a broad high at the Nanawale Estates area to the north, and at Pohoiki on the south. The sharp negative anomalies noted uprift are not observed here. Microearthquake activity is limited to a small zone, perhaps 1.5 by 1.5 miles in size, roughly centered around the successful geothermal wells. Thermal gradient wells are generally warm, less than 500 feet deep, and hence do not offer convincing cutoff information. The Nanawale Estates self potential high occurs in an area of reduced magnetic susceptibility, south of a broad, low amplitude magnetic high.

High steam flow rates and very high temperatures in three successful wells suggest a large volume of cooling magma, probably elongate along the

trend of the rift and along its axis. This low electrical resistivity, weakly magnetized portion of the rift is consistent with extensive fracturing, wall rock alteration, high temperature fluids and/or cooling magma. A northern cutoff to the geothermal reservoir is probably a transitional change in the temperature of subsurface fluids, a function of permeability, and rate of fluid movement. The southern border of the system is obscured in the resistivity data by salt water incursion along the coast. We envision ponding by intact dikes within the rift, and the leakage of fluids down gradient along structures. This would explain the presence of warm seeps along the coast in this area. The southern limit of the reservoir is probably much sharper than the northern limit, and is likely a series of dikes acting as a permeability barrier. Unfortunately these borders are not apparent in the geophysical data. Plate VII presents the interpreted structural features which may act as limits of the reservoir, based on the considerations in this chapter. As in most fracture dominated geothermal systems permeability within the reservoir will be variable and a number of unproductive holes may be drilled which have adequate temperatures. Drill hole L-1, which appears to be favorably sited with respect to electrical resistivity and magnetic features, may be unproductive due to drilling practices or to a local impermeable zone.

SUMMARY AND RECOMMENDATIONS

A detailed aeromagnetic survey of the Kilauea east rift zone has provided a new degree of definition of principal dike zones and transverse structures within the rift zones. In addition several zones of cooling magma, or otherwise high temperature intrusives, have been inferred from sharp magnetic lows along the normally magnetic rift zone.

Numerous observations are noted regarding the ARCO self-potential,

microearthquake, and TDEM resistivity data. These data contribute to a better understanding of both the magnetic data and geothermal potential throughout the rift zone. Unfortunately the known geothermal reservoir is only poorly defined in spite of an extensive geophysical data base, for reasons previously discussed at length. These data coupled with geologic considerations do suggest a substantial area, from one to four square miles (2-10 sq km) as the probable high temperature reservoir area. The nature of the dike complex within this area dictates that low permeability areas are present. These cannot be precisely located with surface geophysical methods at the present time.

Any further interpretation of the data discussed here should focus on a small area, rather than the comprehensive data set. In view of interpretational ambiguities and data density limitations (i.e., the TDEM surveys) it is somewhat doubtful that more definitive interpretation would result. A substantial improvement in the delineation of the known reservoir would require new geologic information, probably from drill results, and possibly from high density electrical surveys and numerical model interpretation. The survey types most likely to offer improved resolution are mise-à-la-masse surveys (i.e. Kauahikaua et al., 1980) and detailed controlled source audio-magnetotelluric (CSAMT). CSAMT data would contribute to reservoir definition if observations could be made to low frequencies of about 0.5 Hz. It would be desirable to discriminate between 3, 6, and 10 ohm-m zones at depths of 3000 to 4000 feet. Additional geophysical studies of this type would be costly and the net improvement in delineating a reservoir at depths below 4000 feet may be marginal. Seismic studies (P-wave attenuation and delay times) for a closely spaced seismometer array centered about the KS-1, KS-2, HGP-A area may provide additional reservoir delineation. The staff at the Hawaiian Volcano

Observatory would probably be the best choice to design and conduct these studies. It may, however, be more appropriate to proceed with step out drilling within the area poorly defined in this report, until more is known about the reservoir.

REFERENCES

Argonaut Enterprises, 1978, Electrical geophysics, Project Area I, Hawaii: report to Atlantic Richfield Co., Dallas, September, 44 p.

Epp, D., and Halunen, A.J., Jr., 1979, Temperature profiles in wells on the island of Hawaii: HIG Report HIG-79-7, 31 p.

Furumoto, A.S., and Kovack, R.L., 1979, The Kalapana earthquake of November 29, 1975: An intra-plate earthquake and its relation to geothermal processes: Physics of the Earth and Planetary Interiors, v. 18, p. 197-208.

Godson, R.H., Zablocki, C.J., Pierce, H.A., Frayser, J.B., Mitchell, C.M., and Sneddon, R.A., 1981, Aeromagnetic map of the island of Hawaii: USGS Geophys. Investigations Map GP-946.

Holcomb, R.T., 1980, Preliminary geologic map of Kilauea Volcano, Hawaii USGS Open File Report.

Kauahikaua, J., and Klein, D., 1978, Results of electrical survey in the arae of Hawaii geothermal test well HGP-A: Geothermal Resources Council Trans., v. 2, p. 363-366.

Kauahikaua, J.P., and Klein, D.P., 1977a, Electromagnetic induction sounding measurements, in HIG-77-15, p. 91-120.

Kauahikaua, J.P., and Klein, D.P., 1977b, Interpretation of electromagnetic transient soundings made on the east rift of Kilauea Volcano, Hawaii: in HIG-77-15, p. 121-174.

Kauahikaua, J., 1981, Interpretation of time-domain electromagnetic soundings in the east rift geothermal area of Kilauea Volcano, Hawaii: USGS Open File report, 81-(draft version), 17 p.

Kauahikaua, J., Mattice, M., and Jackson, D., 1980, Mise-a-la-masse mapping of the HGP-A geothermal reservoir, Hawaii: Geothermal Resources Council Trans., v. 4, p. 65-68.

Keller, G.V., Skokan, C.K., Skokan, J.J., Daniels, J., Kauahikaua, J.P., Klein, D.P., and Zablocki, C.J., 1977a, Geoelectric studies on the east rift, Kilauea Volcano, Hawaii island: HIG report HIG-77-15, 195 p.

Koyanagi, R. Y., 1968, Hawaiian seismic events during 1965: USGS Prof. Paper 600-B, pp. B95-B98.

Koyanagi, R. Y., and Endo, E. T., 1965, Hawaiian seismic events during 1963: USGS Prof. Paper 525-B, pp. B13-B16.

Macdonald, G.A., 1949, Petrography of the island of Hawaii: USGS Prof. Paper 214-D, 96 p.

Mankinen, E.A., and Dalrymple, G.B., 1979, Revised geomagnetic polarity time scale for the interval 0-5 m.y. B.P. JGR, v. 84, no. B2, pp. 615-626.

MicroGeophysics, 1978, Passive seismic survey, Project Area I, Hawaii: report to Atlantic Richfield Co., Dallas, 26 p.

MicroGeophysics, 1978, Composite geophysical interpretation, Project Area I, Hawaii: report to Atlantic Richfield Co., Dallas, 8 p.

MicroGeophysics, 1978, Self potential survey, Project Area I, Hawaii: report to Atlantic Richfield Co., Dallas, 15 p.

Moore, J.G., 1971, Bathymetry and geology-East Cape of the Island of Hawaii: USGS Misc. Inv. Map I-677.

Moore, R.B., 1982, Preliminary geologic map of the Pahoa South quadrangle, Hawaii: Open File report.

Peterson, D.W., 1979, Geologic map of the Kilauea Crater Quadrangle, Hawaii: USGS Map GQ-667.

Ross, H.P., 1982, A review of public geophysical data, Kilauea-east rift area, Hawaii: consulting report to Thermal Power Company, San Francisco, August, 34 p.

Swanson, D.A., Duffield, W.A., and Fiske, R.S., 1976, Displacement of the south flank of Kilauea Volcano: the result of forceful intrusion of magma into the rift zones: USGS Prof. Paper 963, 39 p.

USGS Hawaiian Volcano Observatory, 1983, Special Report-Kilauea Volcano Hawaii: EOS, v. 64, n. 4, p. 25 (Jan. 25).

Zablocki, C.J., 1976, Mapping thermal anomalies on an active volcano by the self-potential method, Kilauea, Hawaii: in Proc. of the Second U.N. Symposium on the development and use of geothermal resources, San Francisco, CA, May 1975, v. 2, pp. 1299-1309.

Zablocki, C.J., 1977, Self-potential studies in East Puna, Hawaii: in HIG-77-15, p. 175-195.

APPENDIX I

NUMERICAL MODEL RESULTS
(Solution for Aeromagnetic Survey Data)

KAPOHO STATE MODEL 4, ITER 5	3-D
KAPOHO STATE MODEL 5, ITER 3	2 1/2-D
KAPOHO CRATER MODEL A, ITER 2	3-D
KAPOHO CRATER MODEL C, ITER 6	3-D
KAPOHO CRATER MODEL D, ITER 3	2 1/2-D
MAGMA AT 5000 FT., ITER 2	3-D
LINE 78, NAPAU COASTLINE AREA, MODEL A	2 1/2-D
LINE 78, NAPAU COASTLINE AREA, MODEL C	2 1/2-D

INPUT PARAMETERS FOR FIGURES IN TEXT

Figure 4b, Transverse fault	3-D
Figure 4c, Rift zone and dikes	3-D
Figure 5a, Lae O Kahuna Coast Profile #1	2 1/2-D
Figure 5b, Lae O Kahuna Coast Profile #1	2 1/2-D
Figure 5c, Line 41, S. Coastline Area, Profile #2	2 1/2-D
Figure 5d, Line 41, S. Coastline Area, Profile #2	2 1/2-D
Figure 8 Puu Kaliu Rift, L-36-L-39	2 1/2-D

KAPOHO STATE MODEL (3-D AND 2 1/2-D)

The magnetic expression near the Kapoho State geothermal system is quite complex. The final model shown here duplicates the contour patterns and amplitudes quite well, and required 31 prisms. Both the transverse structural trend and the localized magnetic highs have been matched. The prism locations and contour patterns are shown at 1:24,000 for the central area and at reduced scale for a larger area. The parameters for each prism are indicated on the printout of the input parameters. It is important to note that the observed data have been matched with prisms which do not extend beyond 4000 feet in depth, i.e. the observed magnetic expression is almost entirely due to the 0-4000 foot depth range.

The magnetic data are also modeled in profile form, using a 2 1/2-D model which accounts for finite strike length, but cannot account for many irregular bodies and off profile bodies. The basic model is taken from the 3-D solution, where a non-magnetic zone occurs within a dipping magnetic body (10,000 μcgs) which terminates at depths of 4000 feet.

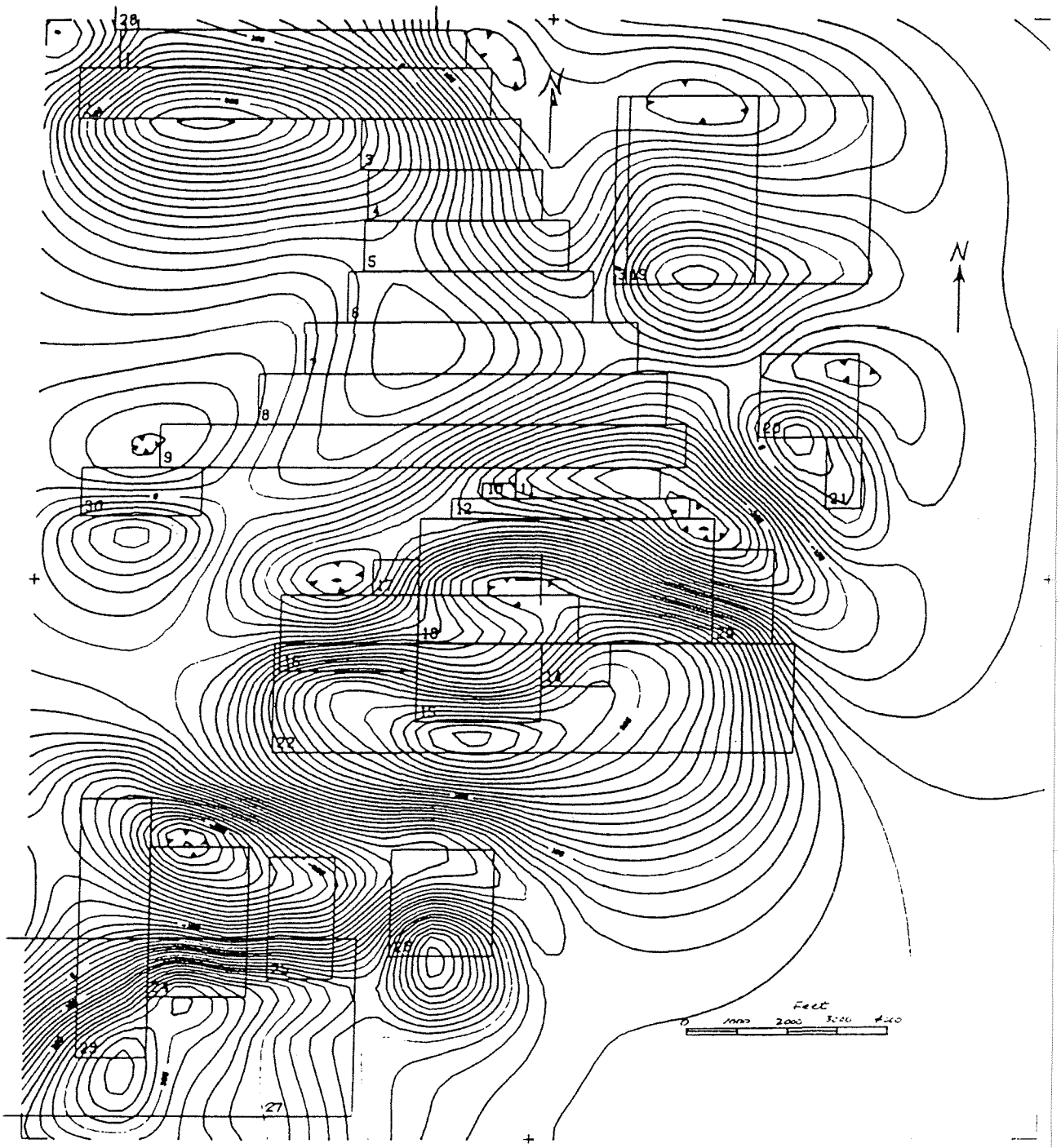

PROJECT NAME

KAPAHO STATE

MODEL NAME

MODEL 4

NUMBER OF PRISMS: 31.

MAGNETIC MODEL (GAMMAS)

GRID PARAMETERS

GRID POINTS X 21. Y 29.

GRID SPACING = 1000. FEET

GRID DIMENSIONS X 20000. Y 22000. FEET

GRID OFFSET X= 0. Y= 0. FEET

SCALE 1:24000.

0 1000 2000 3000 feet

DATA MAXIMUM= 482.

DATA MINIMUM= -982.

CONTOUR INTERVAL 100.

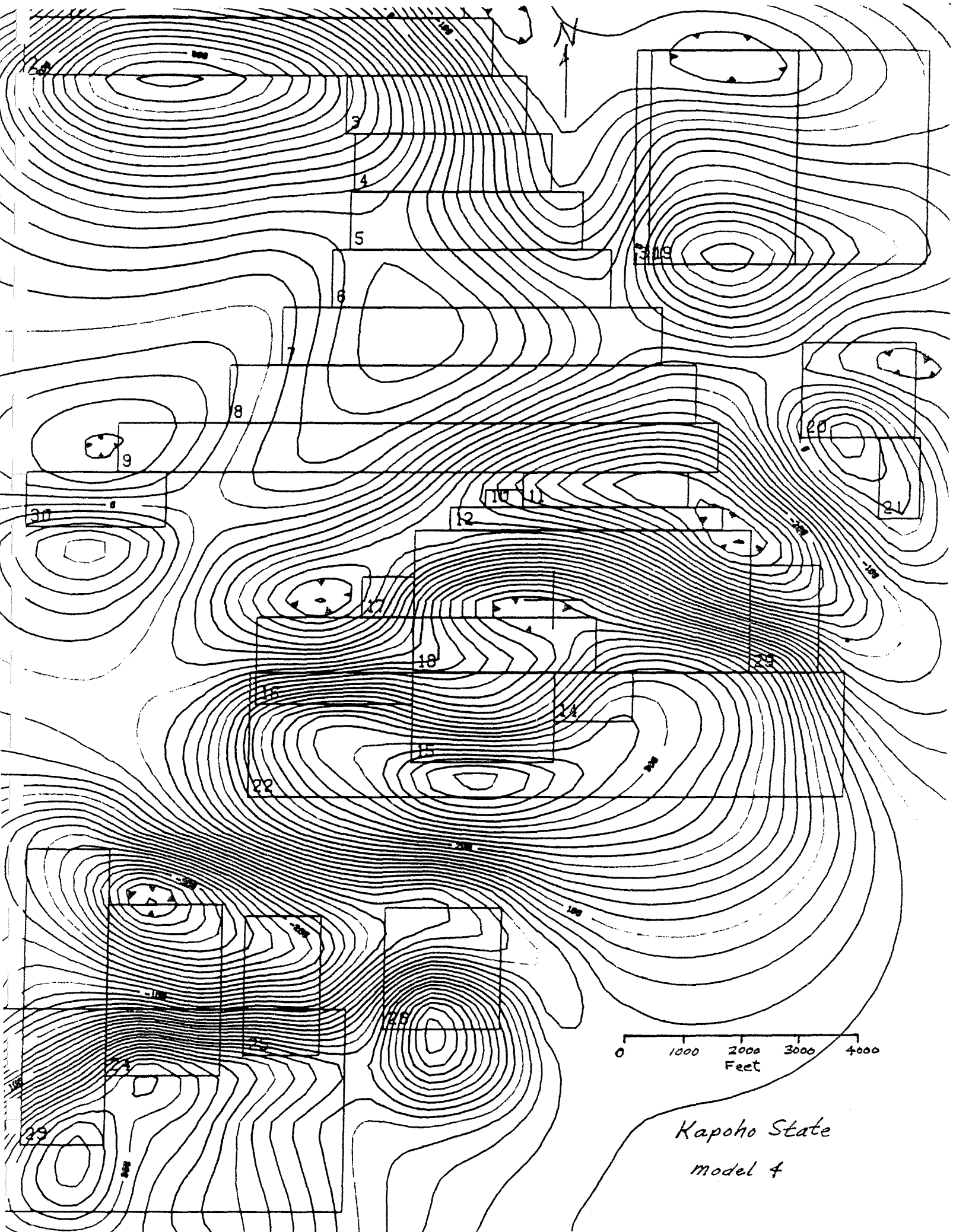
N
3
4
5
6
7
8
9
10
11
12
13
19
20
21
30
17
18
16
24
15
22
23
25
26
27
29
0
1000
2000
3000
4000
Feet
Kapoho State
model 4

F 1 8

Project name: KAPAHU STATE

Model: MODEL 4 Iter #5

MODEL 4, Iter 5
FINAL FIT - 3-D

Units in Feet

MAGNETIC PARAMETERS
Earth"s field: 35000. gammas.
Inclination = 37. degrees Declination = 11. degrees.

PRISM	X1	X2	Y1	Y2	D1	D2	DC	SC
1	-8500.	-1700.	10050.	10800.	800.	3000.	0.00	4000.
2	-9300.	-1200.	9050.	10050.	800.	3000.	0.00	4000.
3	-8700.	-800.	8050.	9050.	1000.	3000.	0.00	4000.
4	-3550.	-150.	7050.	8050.	1200.	3000.	0.00	4000.
5	-3600.	400.	6050.	7050.	1000.	3000.	0.00	4000.
6	-3900.	700.	5050.	6050.	1000.	3000.	0.00	4000.
7	-4750.	1600.	4050.	5050.	1000.	3000.	0.00	3000.
8	-5650.	2400.	3050.	4050.	1000.	3000.	0.00	2000.
9	-7550.	3200.	2200.	3050.	1000.	3000.	0.00	2000.
10	-1200.	-550.	1600.	1900.	800.	4000.	0.00	6000.
11	-550.	2300.	1600.	2200.	800.	4000.	0.00	6000.
12	-1800.	2500.	1200.	1600.	800.	4000.	0.00	6000.
13	-2400.	3400.	-1250.	1200.	800.	4000.	0.00	6000.
14	50.	1400.	-2100.	-1250.	800.	1500.	0.00	6000.
15	-2400.	50.	-2800.	-1250.	800.	1500.	0.00	6000.
16	-5100.	-2400.	-1800.	-300.	800.	4000.	0.00	5000.
17	-3300.	-2400.	-300.	400.	800.	4000.	0.00	5000.
18	-2400.	750.	-1250.	-300.	800.	3000.	0.00	-6000.
19	1550.	4350.	5800.	9500.	1200.	4000.	0.00	2500.
20	4250.	6100.	2800.	4450.	700.	3000.	0.00	4000.
21	5600.	6300.	1400.	2800.	700.	3000.	0.00	4000.

22	-5200.	5150.	-3400.	-1250.	1500.	4000.	0.00	4000.
23	-6950.	-7050.	-9400.	-4300.	500.	2000.	0.00	4000.
24	-7550.	-5400.	-8200.	-5250.	500.	2000.	0.00	6000.
25	-5200.	-3900.	-7850.	-5450.	500.	2000.	0.00	5000.
26	-2600.	-800.	-7400.	-5300.	500.	3000.	0.00	5000.
27	-12600.	-5450.	-10550.	-7050.	2000.	5000.	0.00	5000.
28	-8600.	-2300.	10600.	14100.	800.	5000.	0.00	4000.
29	3400.	4600.	-1250.	600.	800.	4000.	0.00	6000.
30	-9100.	-6700.	1250.	2200.	800.	3000.	0.00	4000.
31	1300.	4100.	5600.	9100.	600.	1200.	0.00	2500.

RID PARAMETERS

Magnetic Model

Number of Grid Points in X Direction: 21

Number of Grid Points in Y Direction: 23

Grid Spacing in Feet: 1000.00

X Offset in Feet: 0.00

Y Offset in Feet: 0.00

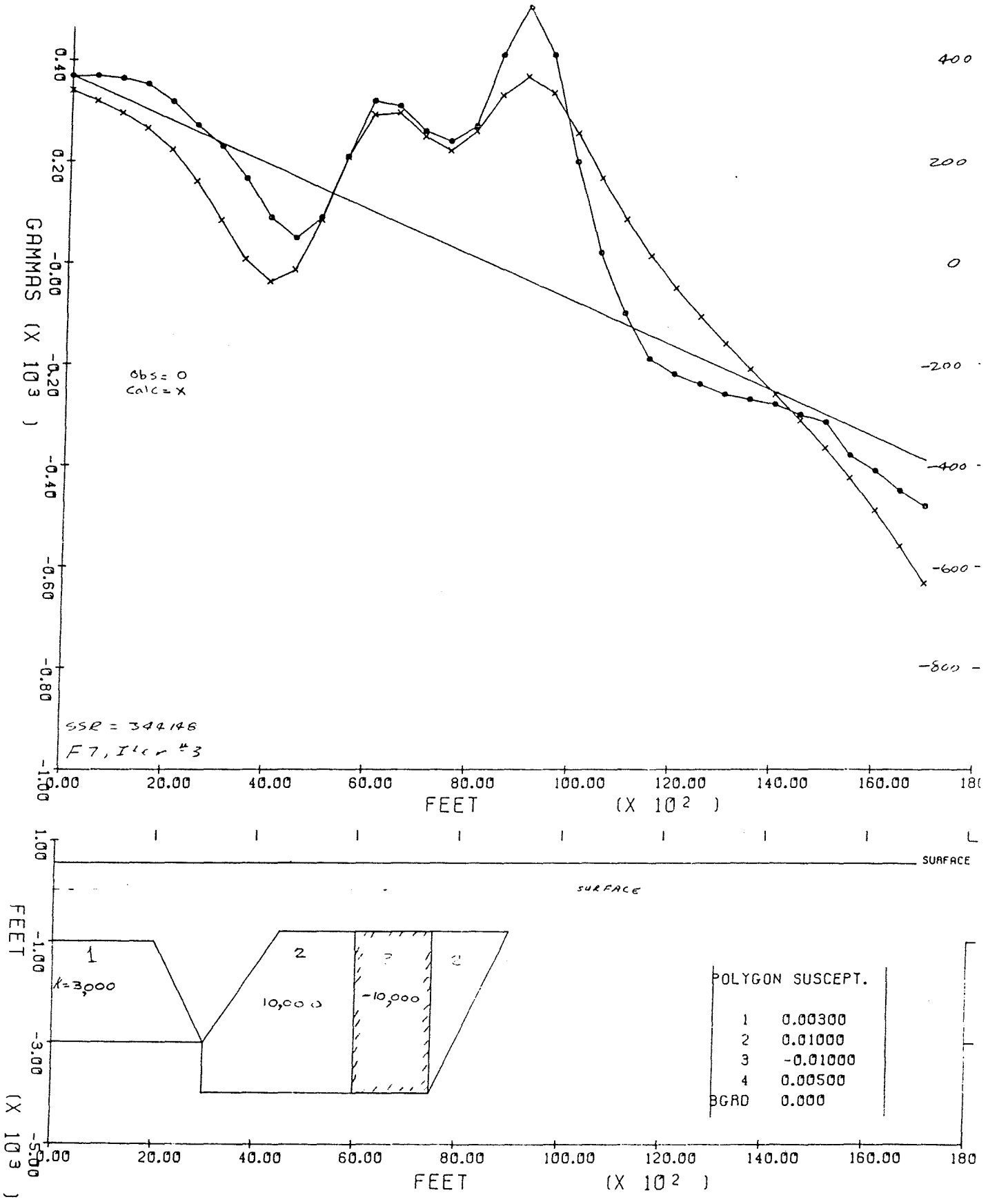

KAPAHO STATE 2½ D MODEL

F7

Work File Header: RIFT STUDY
Earth's total magnetic field (gammas) = 35850.000
Inclination (deg.) of earth's total field = 37.0000
Angle (deg.) from magnetic north to profile axis = 161.0000

NOTE: The printed results are from a previous model
This model has not been executed

The total sum of squares is 344146.313
Units of distance for this model = FEET
Meters per unit of distance = 0.305
Number of inches per unit of distance = 12.000
The Current map scale is set to 1.

KAPOHO STATE
2½-D

* Station Data *

F7

Profile Id: KAPOHO STATE

Station	Distance to Station	Elev.	Observed Magnetic	Calc. Magnetic	Anomaly	Total Magnetic	Diff. ANM-MAG
1	0.000	550.000	370.00	340.87	0.00	-29.13	29.13
2	500.000	550.000	370.00	319.96	22.33	-27.71	50.04
3	1000.000	550.000	365.00	295.92	39.67	-29.41	69.08
4	1500.000	550.000	353.00	266.02	50.00	-36.98	86.98
5	2000.000	550.000	318.00	223.50	37.33	-57.17	94.50
6	2500.000	550.000	272.00	181.74	13.67	-96.60	110.26
7	3000.000	550.000	230.00	84.19	-6.00	-151.81	145.81
8	3500.000	550.000	167.00	8.13	-46.67	-205.54	158.87
9	4000.000	550.000	90.00	-36.20	-101.33	-227.53	126.20
10	4500.000	550.000	50.00	-12.92	-119.00	-181.92	62.92
11	5000.000	550.000	90.00	84.32	-56.67	-62.34	5.66
12	5500.000	550.000	210.00	208.69	65.67	84.35	1.31
13	6000.000	550.000	320.00	292.46	218.00	190.46	27.54
14	6500.000	550.000	310.00	296.09	230.33	216.43	13.91
15	7000.000	550.000	260.00	248.87	202.67	191.54	11.13
16	7500.000	550.000	240.00	221.68	205.00	186.68	18.32
17	8000.000	550.000	270.00	259.00	257.33	246.33	11.00
18	8500.000	550.000	410.00	330.72	419.67	340.39	79.28
19	9000.000	550.000	510.00	367.64	542.00	399.64	142.36
20	9500.000	550.000	410.00	354.82	464.33	389.15	75.18
21	10000.000	550.000	200.00	256.35	276.67	333.02	-56.35
22	10500.000	550.000	20.00	167.73	119.00	266.73	-147.73
23	11000.000	550.000	-100.00	85.56	21.33	206.89	-185.56
24	11500.000	550.000	-190.00	13.32	-46.33	156.98	-203.32
25	12000.000	550.000	-220.00	-50.18	-54.00	115.82	-169.82
26	12500.000	550.000	-240.00	-107.20	-51.67	81.14	-132.80
27	13000.000	550.000	-260.00	-159.98	-49.33	50.69	-100.02
28	13500.000	550.000	-270.00	-210.53	-37.00	22.47	-59.47
29	14000.000	550.000	-280.00	-260.64	-24.67	-5.31	-19.36
30	14500.000	550.000	-300.00	-311.96	-22.33	-34.29	11.96
31	15000.000	550.000	-315.00	-366.08	-15.00	-66.08	51.08
32	15500.000	550.000	-380.00	-424.54	-57.67	-102.21	44.54
33	16000.000	550.000	-410.00	-488.65	-65.33	-143.98	78.65
34	16500.000	550.000	-450.00	-558.77	-83.00	-191.77	108.77
35	17000.000	550.000	-480.00	-632.63	-90.67	-243.30	152.63

* Model Data *

Background susceptibility = 0.00000

5

Polygon no. 1 Susceptibility = 0.00300
Strike half length = 4000.00000

X-vertice	Z-vertice
-4000.000	1000.000
2000.000	1000.000
3000.000	3000.000
-4000.000	3000.000
-4000.000	1000.000

Kapoho State
2½ D

Polygon no. 2 Susceptibility = 0.01000
Strike half length = 3000.00000

X-vertice	Z-vertice
4500.000	800.000
~~9000.000~~	800.000
7500.000	4000.000
3000.000	4000.000
-3000.000	3000.000
4500.000	800.000

(with suggested changes for another iteration)

Polygon no. 3 Susceptibility = -0.01000
Strike half length = 1700.00000

X-vertice	Z-vertice
6000.000	800.000
7500.000	800.000
7500.000	4000.000
6000.000	4000.000
6000.000	800.000

Polygon no. 4 Susceptibility = 0.00500
Strike half length = 8000.00000

X-vertice	Z-vertice
18000.000	1000.000
26000.000	1000.000
26000.000	5000.000
18000.000	5000.000
18000.000	1000.000

* Regional data *

Left regional - X = 0.000
Left regional - mag.intens. = 370.000
Right regional - X = 15000.000
Right regional - mag.intens. = -300.000

Regional values for current station locations

	Station dis.	Regional
1	0.000	370.000
2	500.000	347.667
3	1000.000	325.333
4	1500.000	303.000
5	2000.000	280.667

KAPOHO CRATER MODEL (3-D AND 2 1/2-D)

Model A attempts to simulate the 1:24,000 map contours for the Kapoho Crater area with 7 positive sources. Even the topography of the crater rim and interior are modeled to a first approximation, but these have a small effect on the computed anomaly. The contour pattern has little resemblance to the observed data, and the strong minimum lies north of the main maximum, opposite to the observed data.

Model C is a second effort using a large positive prism to represent the island itself, with two negative susceptibility prisms in the crater area. The effect of the negative susceptibility superimposed on the positive background is to give an area of low ($\sim$ 0) susceptibility. The result is a good fit to the observed contours, with the large closed low south of the maximum. Kapoho Crater is centered over prism 2, the low susceptibility area.

Model D is a 2 1/2-D model of a profile across Kapoho Crater, computed in a further effort to verify the low susceptibility nature of the rock beneath the crater. A simple model duplicates the north maximum-south minimum character of the observed anomaly although the regional gradient is not fully accounted for. An excellent fit would result from an adjustment of the regional and raising the background susceptibility to +16,000 microcgs. The models leave little doubt that the crater area is either near zero susceptibility or possibly reversely magnetized.

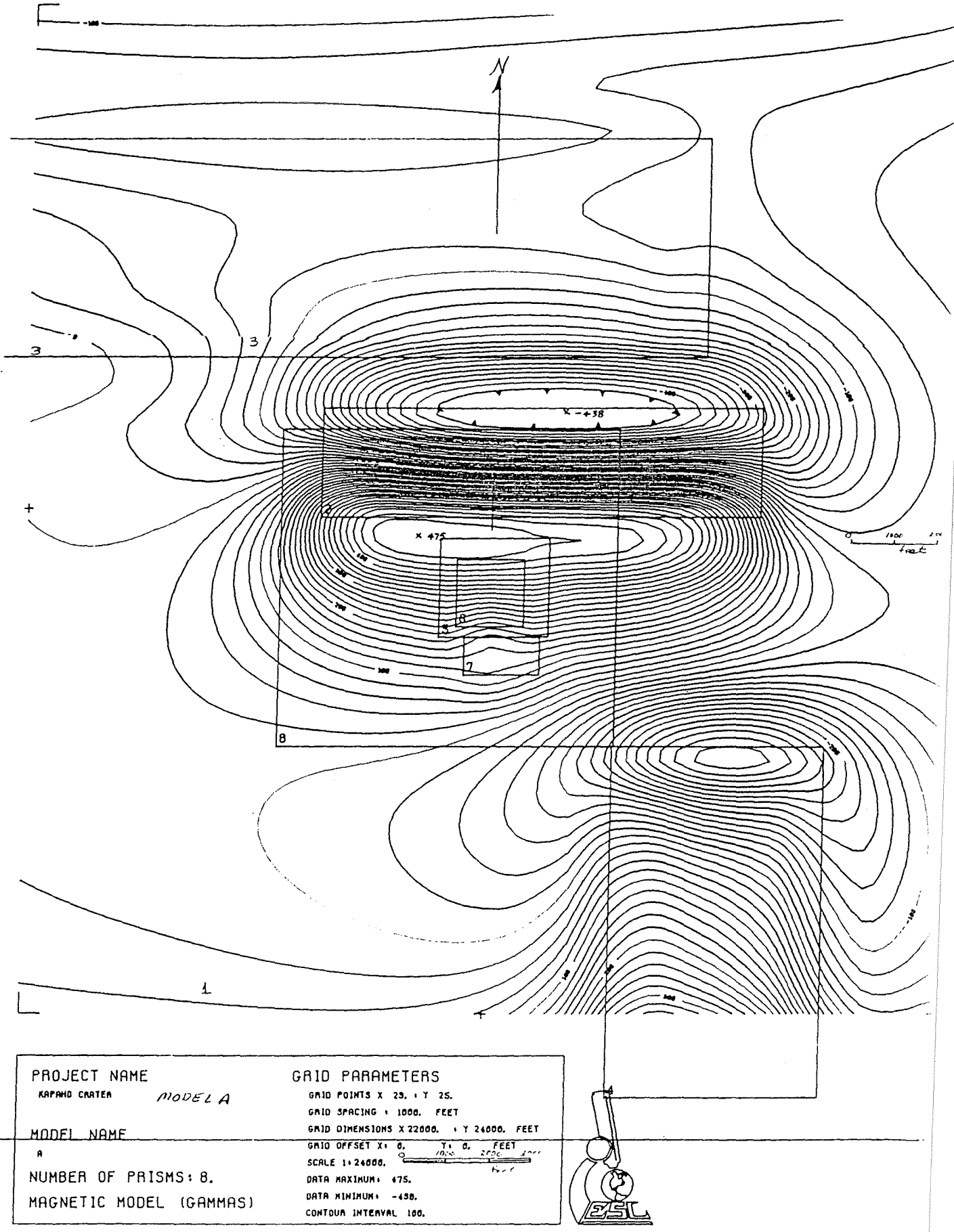

PROJECT NAME

KAPAHO CRATER MODEL A

MODEL NAME

A

NUMBER OF PRISMS: 8.

MAGNETIC MODEL (GAMMAS)

GRID PARAMETERS

GRID POINTS X 29. Y 25.

GRID SPACING : 1000. FEET

GRID DIMENSIONS X 22000. Y 24000. FEET

GRID OFFSET X: 0. Y: 0. FEET

SCALE 1:24000.

DATA MAXIMUM: 475.

DATA MINIMUM: -438.

CONTOUR INTERVAL 100.

Project name: KAPAHO CRATER

Model: A

MODEL A, ITER 2
(with suggested changes for next iter)

Units in Feet

MAGNETIC PARAMETERS
Earth"s field: 35000. gammas.
Inclination = 37. degrees Declination = 11. degrees.

PRISM	X1	X2	Y1	Y2	D1	D2	DC	SC
1	-20000.	14000.	-15000.	14000.	550.	~~5000.~~	0.00	~~1500.~~
2	-4060.	~~6400.~~	-200.	2400.	1000.	5000.	0.00	~~8000.~~
3	-14000.	5050.	3000.	~~8600.~~	500.	1000.	0.00	~~1000.~~
4	2950.	~~8600.~~	~~-14000.~~	~~-5650.~~	1000.	5000.	0.00	~~6000.~~
5	-1200.	1400.	-3050.	-700.	450.	550.	0.00	2500.
6	-800.	800.	-2800.	-1200.	450.	600.	0.00	-2500.
7	-600.	1200.	-3950.	-3050.	450.	550.	0.00	2500.
8	-5000.	~~5100.~~	~~-5650.~~	1900.	3000.	5000.	0.00	~~-1500.~~

GRID PARAMETERS
Magnetic Model
Number of Grid Points in X Direction: 23
Number of Grid Points in Y Direction: 25
Grid Spacing in Feet: 1000.00
X Offset in Feet: 0.00
Y Offset in Feet: 0.00

Prism 1 K 7000

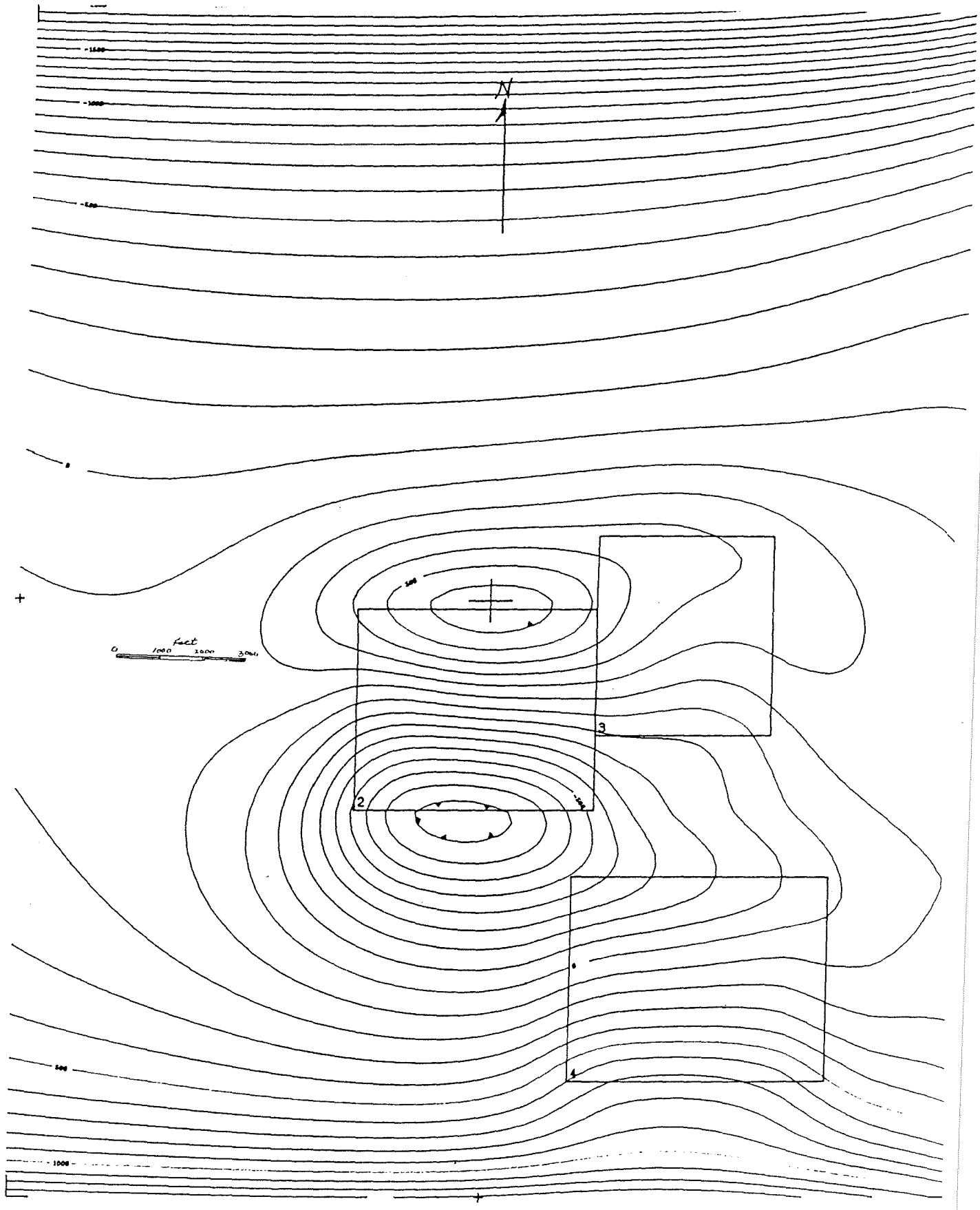

PROJECT NAME

KAPAHO CRATER

MODEL C

MODEL NAME

A

NUMBER OF PRISMS: 4.

MAGNETIC MODEL (GAMMAS)

GRID PARAMETERS

GRID POINTS X 23. Y 29.

GRID SPACING 1000. FEET

GRID DIMENSIONS X 22000. Y 28000. FEET

GRID OFFSET X: 0. Y: 0. FEET

SCALE 1:24000.

DATA MAXIMUM: 1398.

DATA MINIMUM: -2068.

CONTOUR INTERVAL 500.

Project name: KAPOHO CRATER

Model: C

Units in Feet

Model C
Kapoho Crater
Good fit with low or -ve susc bod

MAGNETIC PARAMETERS
Earth"s field: 35850. gammas.
Inclination = 37. degrees Declination = 11. degrees.

PRISM	X1	X2	Y1	Y2	D1	D2	DC	SC
1	-20000.	14100.	-15100.	14100.	550.	8000.	0.00	12000.
2	-3100.	2500.	-4950.	-200.	1500.	5000.	0.00	-15400.
3	2500.	6600.	-3200.	1500.	1500.	5000.	0.00	-6400.
4	2000.	8000.	-11300.	-6500.	1000.	5000.	0.00	4000.

GRID PARAMETERS
Magnetic Model
Number of Grid Points in X Direction: 23
Number of Grid Points in Y Direction: 29
Grid Spacing in Feet: 1000.00
X Offset in Feet: 0.00
Y Offset in Feet: 0.00

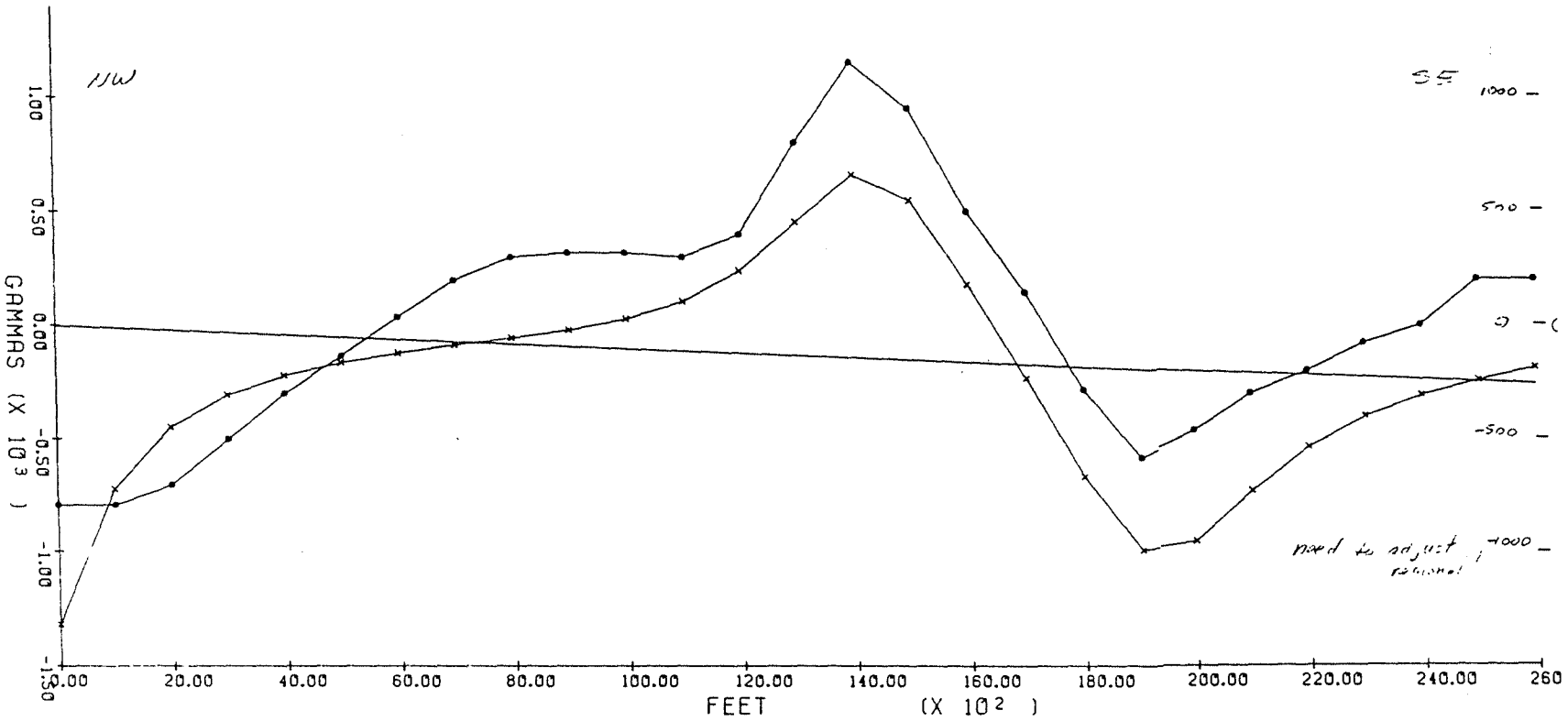

OBSERVED= ⊙
CALCULATED= X

POLYGON	SUSCEPT.
1	0.01200
2	-0.01600
BGRD	0.000

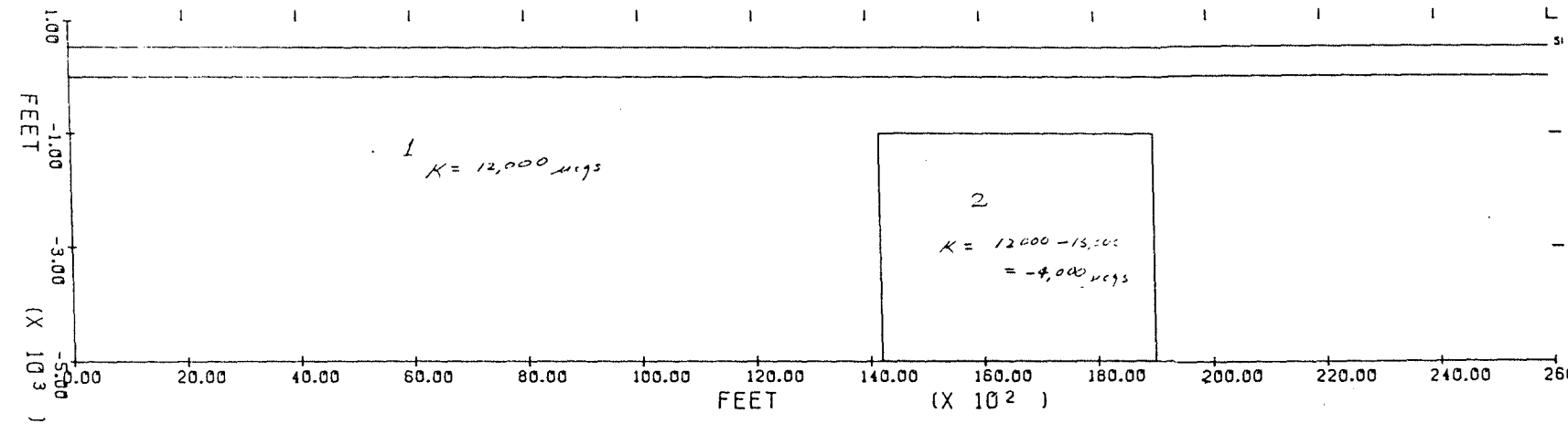

KAPAHO CRATER Model D

Work File Header: RIFT STUDY
Earth's total magnetic field (gammas) = 35850.000
Inclination (deg.) of earth's total field = 37.0000
Angle (deg.) from magnetic north to profile axis = 179.0000

OTE: The printed results are from a previous model
This model has not been executed

MODEL D
KAPOHO CRATER 2½.
first approximation
-ve susc or zero body

he total sum of squares is 3044480.500
nits of distance for this model = FEET
Meters per unit of distance = 0.305
Number of inches per unit of distance = 12.000
he Current map scale is set to 1.

* Station Data *

F-9

rofile Id: KAPOHO CRATER

Station	Distance to Station	Elev.	Observed Magnetic	Calc. Magnetic	Anomaly	Total Magnetic	Diff. ANM-MAG
1	0.000	530.000	-790.00	-1318.10	-790.00	-1318.10	528.10
2	1000.000	530.000	-790.00	-718.65	-780.00	-708.65	-71.35
3	2000.000	530.000	-700.00	-446.80	-680.00	-426.80	-253.20
4	3000.000	530.000	-500.00	-306.31	-470.00	-276.31	-193.69
5	4000.000	530.000	-300.00	-219.63	-260.00	-179.63	-80.37
6	5000.000	530.000	-130.00	-160.68	-80.00	-110.68	30.68
7	6000.000	530.000	40.00	-117.49	100.00	-57.49	157.49
8	7000.000	530.000	200.00	-82.95	270.00	-12.95	282.95
9	8000.000	530.000	300.00	-51.38	380.00	28.62	351.38
10	9000.000	530.000	320.00	-16.36	410.00	73.64	336.36
11	10000.000	530.000	320.00	31.54	420.00	131.54	288.46
12	11000.000	530.000	300.00	108.31	410.00	219.31	191.69
13	12000.000	530.000	400.00	240.33	520.00	360.33	159.67
14	13000.000	530.000	800.00	453.46	930.00	583.46	346.54
15	14000.000	530.000	1150.00	659.48	1290.00	799.48	490.52
16	15000.000	530.000	950.00	549.95	1100.00	699.95	400.05
17	16000.000	530.000	500.00	182.83	660.00	342.83	317.17
18	17000.000	530.000	150.00	-230.44	320.00	-60.44	380.44
19	18000.000	530.000	-280.00	-661.05	-100.00	-481.05	381.05
20	19000.000	530.000	-580.00	-988.82	-390.00	-798.82	408.82
21	20000.000	530.000	-460.00	-951.33	-260.00	-751.33	491.33
22	21000.000	530.000	-300.00	-730.36	-90.00	-520.36	430.36
23	22000.000	530.000	-200.00	-536.32	20.00	-316.32	336.32
24	23000.000	530.000	-80.00	-401.06	150.00	-171.06	321.06
25	24000.000	530.000	0.00	-309.79	240.00	-69.79	309.79
26	25000.000	530.000	200.00	-244.21	450.00	5.79	444.21
27	26000.000	530.000	200.00	-187.35	460.00	72.65	387.35

* Model Data *

Background susceptibility = 0.00000

Polygon no. 1 Susceptibility = 0.01200
Strike half length = 14000.000

X-vertice	Z-vertice
0.000	0.000
29000.000	0.000

39000.000	6000.000
-8000.000	6000.000
0.000	0.000

Polygon no. 2 Susceptibility = -0.01600
Strike half length = 3000.00000

X-vertice	Z-vertice
14200.000	1000.000
19000.000	1000.000
19000.000	5000.000
14200.000	5000.000
14200.000	1000.000

Kapoho Crater 2½D

* Regional Data *

Left regional - X = 0.000
Left regional - mag.intens. = 0.000
Right regional - X = 40000.000
Right regional - mag.intens. = -400.000

Regional values for current station locations

	Station dis.	Regional
1	0.000	0.000
2	1000.000	-10.000
3	2000.000	-20.000
4	3000.000	-30.000
5	4000.000	-40.000
6	5000.000	-50.000
7	6000.000	-60.000
8	7000.000	-70.000
9	8000.000	-80.000
10	9000.000	-90.000
11	10000.000	-100.000
12	11000.000	-110.000
13	12000.000	-120.000
14	13000.000	-130.000
15	14000.000	-140.000
16	15000.000	-150.000
17	16000.000	-160.000
18	17000.000	-170.000
19	18000.000	-180.000
20	19000.000	-190.000
21	20000.000	-200.000
22	21000.000	-210.000
23	22000.000	-220.000
24	23000.000	-230.000
25	24000.000	-240.000
26	25000.000	-250.000
27	26000.000	-260.000

MAGMA AT 5000 FEET

This model simulates a magnetic portion of the dike complex which trends northeast (bodies 2-11) with susceptibility of 4000 microcgs (body 1-). Body 12 represents an area where the 4000 microcgs of the lavas has been destroyed below 5000 feet depths by heating to above Curie Point temperatures. It would be hard to interpret the presence of the deep "magma" in the presence of the strong positive, shallow, dike source.

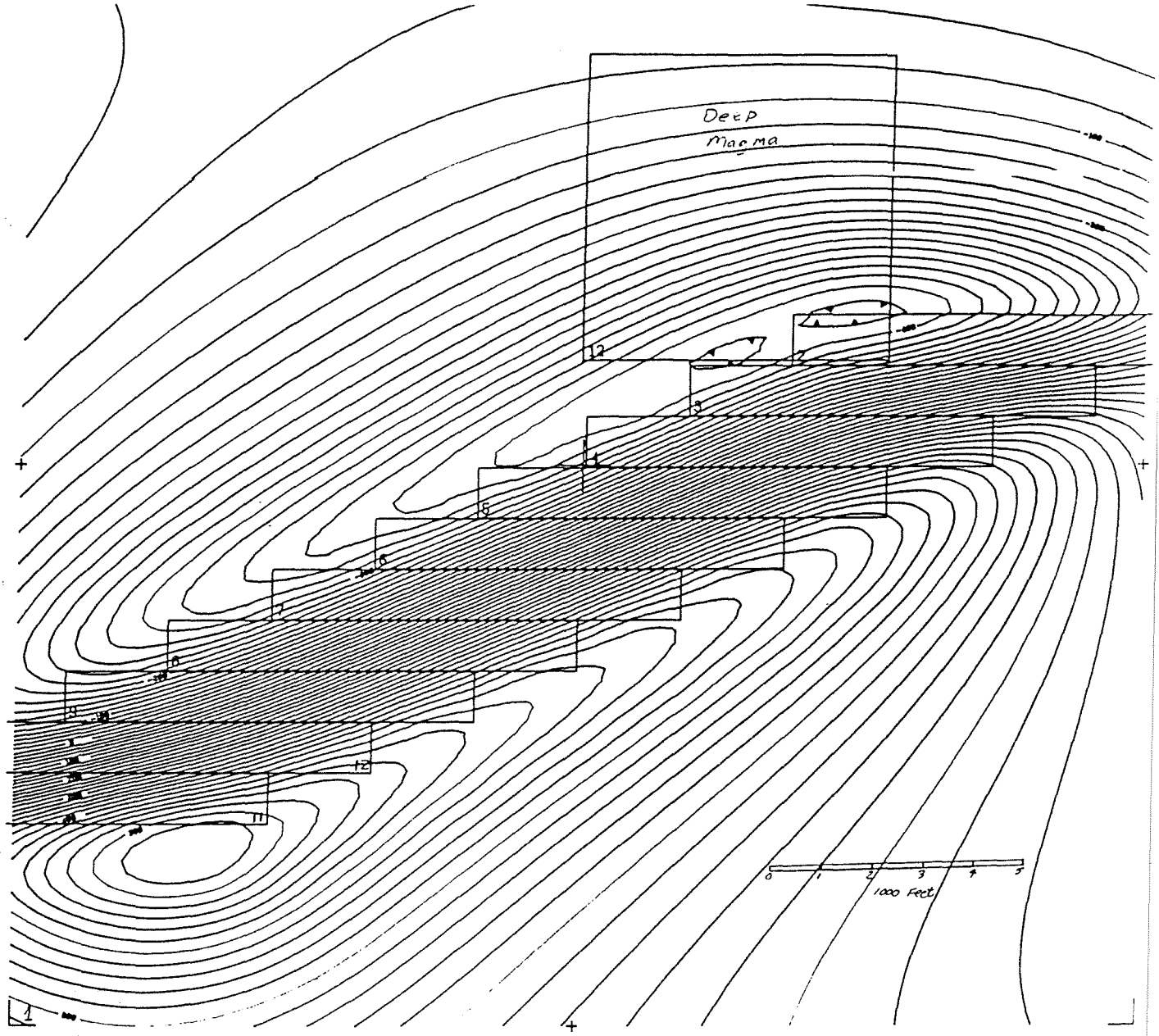

PROJECT NAME

MAGMA AT D= 5000 FT

MODEL NAME

MAGMA @ 5000 FT.

NUMBER OF PRISMS: 12.

MAGNETIC MODEL (GAMMAS)

GRID PARAMETERS

GRID POINTS X 25. Y 25.

GRID SPACING : 1000. FEET

GRID DIMENSIONS X 22000. : Y 22000. FEET

GRID OFFSET X: 0. Y: 0. FEET

SCALE 1:24000. 0 1000 2000 3000 Feet

DATA MAXIMUM: 532.

DATA MINIMUM: -427.

CONTOUR INTERVAL 100.

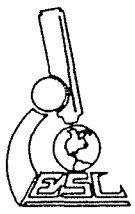

Project name: MAGMA

Model: MAGMA @ 5000 FT.

Units in Feet

MAGNETIC PARAMETERS
Earth"s field: 35850. gammas.
Inclination = 37. degrees Declination = 11. degrees.

PRISM	X1	X2	Y1	Y2	D1	D2	DC	SC
1	-20000.	20000.	-20000.	20000.	550.	10000.	0.00	4000.
2	4050.	12050.	1950.	2950.	1550.	10000.	0.00	4000.
3	2050.	10050.	950.	1950.	1550.	10000.	0.00	4000.
4	50.	8050.	-50.	950.	1550.	10000.	0.00	4000.
5	-2050.	5950.	-1050.	-50.	1550.	10000.	0.00	4000.
6	-4050.	3950.	-2050.	-1050.	1550.	10000.	0.00	4000.
7	-6050.	1950.	-3050.	-2050.	1550.	10000.	0.00	4000.
8	-8050.	-50.	-4050.	-3050.	1550.	10000.	0.00	4000.
9	-10050.	-2050.	-5050.	-4050.	1550.	10000.	0.00	4000.
10	-12050.	-4050.	-6050.	-5050.	1550.	10000.	0.00	4000.
11	-14050.	-6050.	-7050.	-6050.	1550.	10000.	0.00	4000.
12	-50.	5950.	2050.	8050.	5000.	10000.	0.00	-4000.

GRID PARAMETERS
Magnetic Model
Number of Grid Points in X Direction: 23
Number of Grid Points in Y Direction: 23
Grid Spacing in Feet: 1000.00
X Offset in Feet: 0.00
Y Offset in Feet: 0.00

LINE 78 NAPAU COASTLINE AREA (2 1/2-D MODEL)

The observed magnetic profile along flight line 78 models the coastline magnetic anomaly southeast of Napau Crater. Model A simulates a uniformly magnetic (K = 5,000 μcgs) horizon (lavas) on land and a steeply dipping ocean floor. The computed anomaly has much lower amplitude, is displaced to the southeast, and decreases to the southeast much more slowly than the observed anomaly.

Model C is a second attempt at a more complex model. The dipping sea floor has a low susceptibility (K = 1,000), and a wide, vertical magnetic dikelike body (K = 11,000) occurs just inland from the coastline. Lavas north of the dike are more magnetic than those in the sea floor. The fit to the observed data is poor, but much better than model A, clearly indicating that a steeply dipping magnetic dike-like body is present. Several days of computer breakdown interrupted the modeling at this point and modeling was discontinued. A single dike dipping about 55° inland, K = 10,000 μcgs and about 3000 feet wide would better approximate the observed data. An additional magnetic body north of the dike is required.

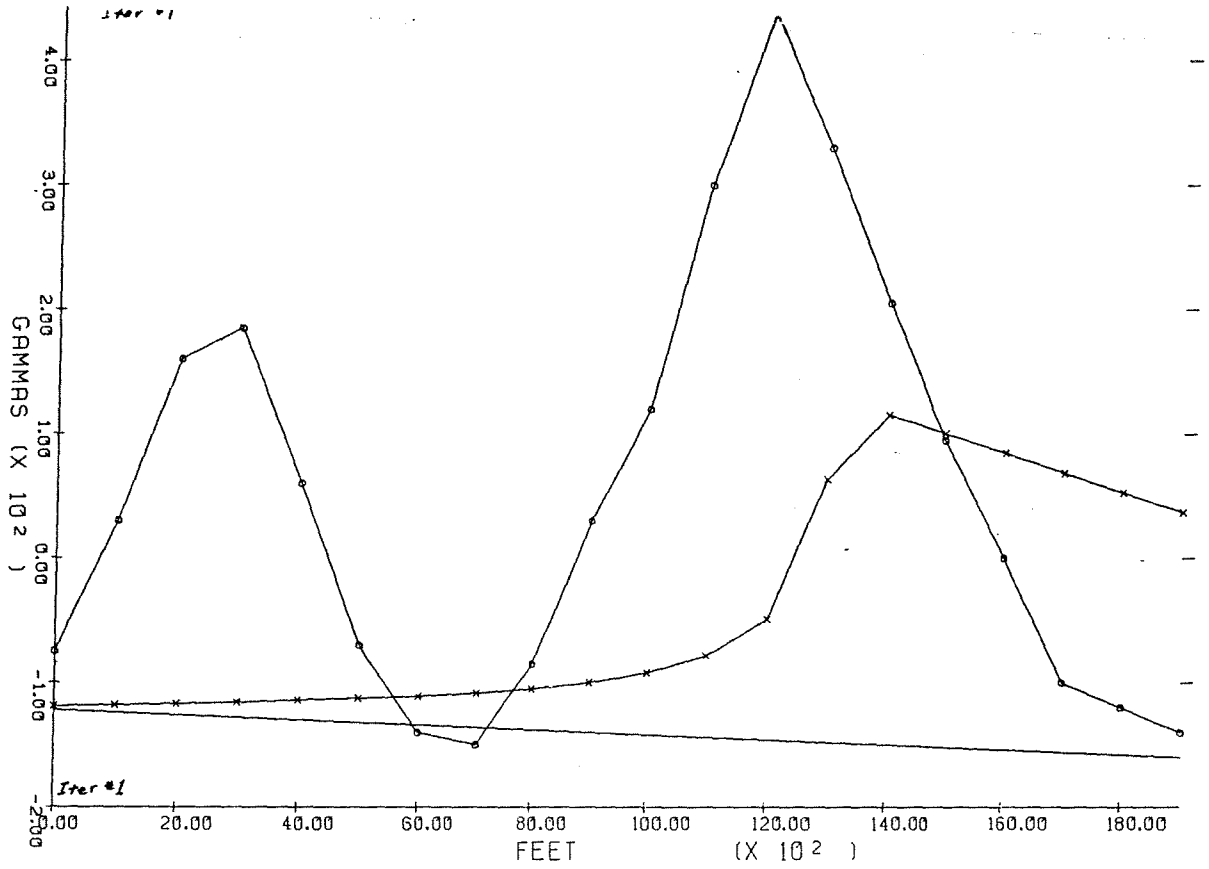

OBSERVED= ⊙
CALCULATED= ×

POLYGON	SUSCEPT.
1	0.00500
BGRD	0.000

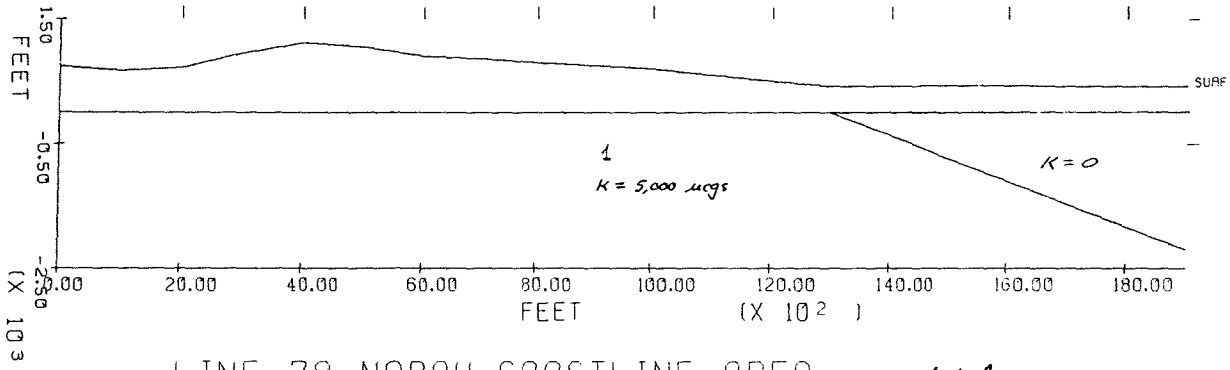

LINE 78 NAPAU COASTLINE AREA *model A*

work File Header: RIFT STUDY
Earth's total magnetic field (gammas) = 35850.000
Inclination (deg.) of earth's total field = 37.0000
Angle (deg.) from magnetic north to profile axis = 135.0000

OTE: The printed results are from a previous model
This model has not been executed

The total sum of squares is 845773.500
nits of distance for this model = FEET
meters per unit of distance = 0.305
Number of inches per unit of distance = 12.000
ne Current map scale is set to 1.

* Station Data *

Model A

rofile Id: LINE 78 NAPAU COASTLINE AREA

Station	Distance to Station	Elev.	Observed Magnetic	Calc. Magnetic	Anomaly	Total Magnetic	Diff. ANM-MAG
1	0.000	740.000	-75.00	-119.02	47.00	2.98	44.02
2	1000.000	670.000	30.00	-117.81	154.00	6.19	147.81
3	2000.000	720.000	160.00	-116.89	286.00	9.11	276.89
4	3000.000	950.000	185.00	-115.79	313.00	12.22	300.78
5	4000.000	1120.000	60.00	-114.24	190.00	15.76	174.24
6	5000.000	1050.000	-70.00	-112.69	62.00	19.31	42.69
7	6000.000	900.000	-140.00	-111.12	-6.00	22.88	-28.88
8	7000.000	860.000	-150.00	-108.60	-14.00	27.40	-41.40
9	8000.000	800.000	-85.00	-105.17	53.00	32.83	20.17
10	9000.000	750.000	30.00	-99.99	170.00	40.01	129.99
11	10000.000	700.000	120.00	-91.77	262.00	50.23	211.77
12	11000.000	600.000	300.00	-78.43	444.00	65.57	378.43
13	12000.000	500.000	440.00	-49.02	586.00	96.98	489.02
14	13000.000	420.000	330.00	63.74	478.00	211.74	266.26
15	14000.000	425.000	205.00	114.76	355.00	264.76	90.24
16	15000.000	435.000	95.00	100.36	247.00	252.36	-5.36
17	16000.000	430.000	0.00	84.43	154.00	238.43	-84.43
18	17000.000	420.000	-100.00	68.59	56.00	224.59	-168.59
19	18000.000	420.000	-120.00	52.45	38.00	210.45	-172.45
20	19000.000	420.000	-140.00	36.79	20.00	196.79	-176.79

* Model Data *

Background susceptibility = 0.00000

Polygon no. 1 Susceptibility = 0.00500
Strike half length = 20000.000

X-vertice	Z-vertice
-15000.000	0.000
13000.000	0.000
19000.000	2200.000
29000.000	4000.000
33000.000	6000.000
-15000.000	6000.000
-15000.000	0.000

* Regional Data *

Rev on 5

Left regional - X = -1000.000
Left regional - mag.intens. = -120.000
Right regional - X = 19000.000
Right regional - mag.intens. = -160.000

Regional values for current station locations

	Station dis.	Regional
1	0.000	-122.000
2	1000.000	-124.000
3	2000.000	-126.000
4	3000.000	-128.000
5	4000.000	-130.000
6	5000.000	-132.000
7	6000.000	-134.000
8	7000.000	-136.000
9	8000.000	-138.000
10	9000.000	-140.000
11	10000.000	-142.000
12	11000.000	-144.000
13	12000.000	-146.000
14	13000.000	-148.000
15	14000.000	-150.000
16	15000.000	-152.000
17	16000.000	-154.000
18	17000.000	-156.000
19	18000.000	-158.000
20	19000.000	-160.000

Model A

Poly No. 2 # sides, susc, Y(2) = 4; 5000; 7,000

XSTART, ZSTART (1) -7,000, 0
(2) +9,500, 0
(3) +9,500, 5000
(4) -7,000, 5000
(5) -7,000, 0

Poly No. 3 # sides, susc, Y(3) = 5; 10,000; 12,000

XSTART, ZSTART (1) 7000, 500
(2) 12,000, 500
(3) 12,000, 5000
(4) 7000, 5000
(5) 7000, 500

Suggested changes for next iteration.

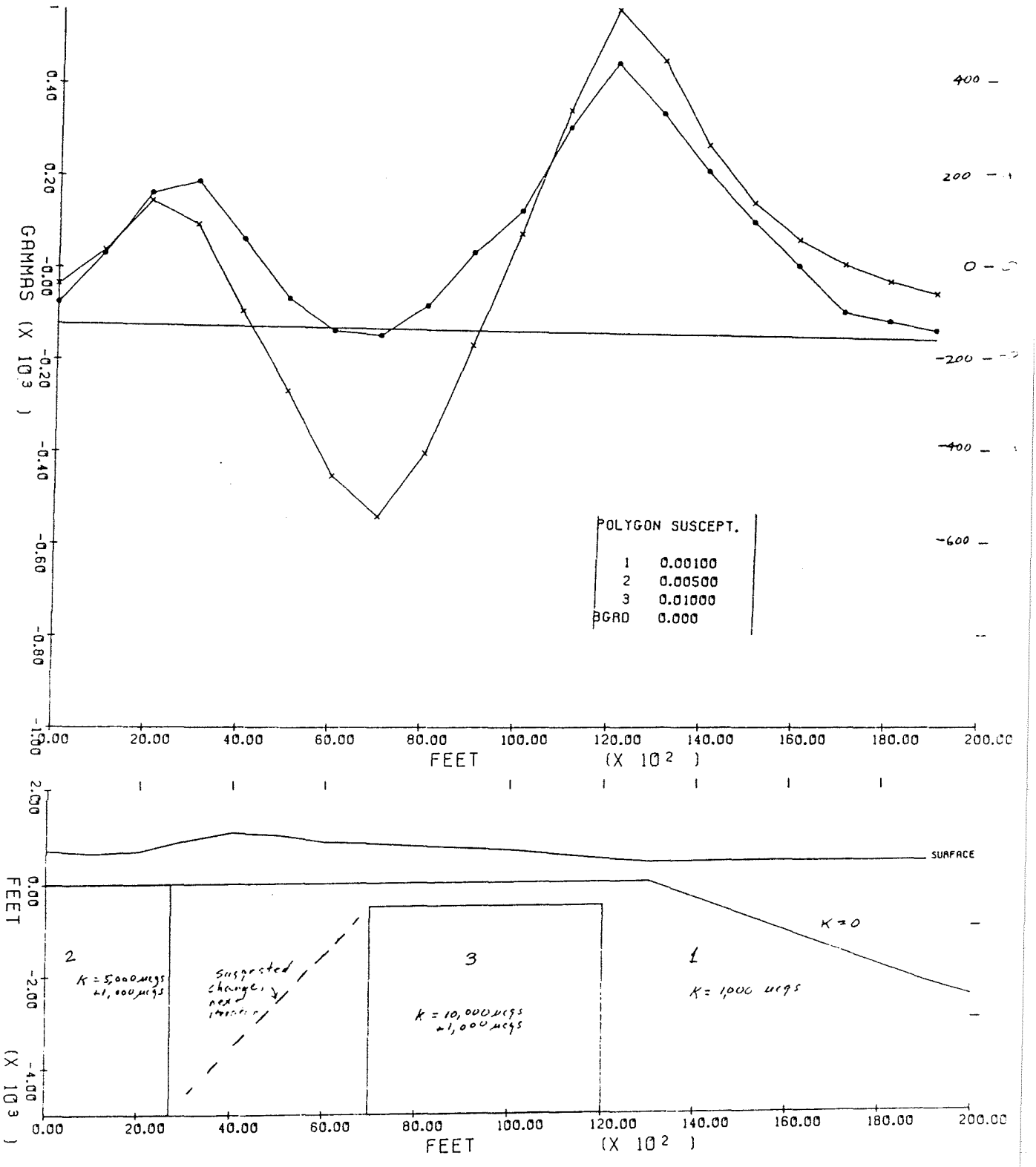

LINE 78 NAPAU COASTLINE AREA *model C*

F8

Work File Header: RIFT STUDY
Earth's total magnetic field (gammas) = 35850.000
Inclination (deg.) of earth's total field = 37.0000
Angle (deg.) from magnetic north to profile axis = 135.0000

NOTE: The printed results are from a previous model
This model has not been executed

The total sum of squares is 534713.675
Units of distance for this model = FEET
Meters per unit of distance = 0.305
Number of inches per unit of distance = 12.000
The Current map scale is set to 1.

Model C

F8

* Station Data *

Profile Id: LINE 78 NAPAU COASTLINE AREA

Station	Distance to Station	Elev.	Observed Magnetic	Calc. Magnetic	Anomaly	Total Magnetic	Diff. ANM-MAG
1	0.000	740.000	-75.00	-34.60	47.00	87.40	-40.40
2	1000.000	670.000	30.00	37.82	154.00	161.82	-7.82
3	2000.000	720.000	160.00	142.94	286.00	268.94	17.06
4	3000.000	950.000	185.00	91.27	313.00	219.27	93.73
5	4000.000	1120.000	60.00	-96.59	190.00	33.41	156.59
6	5000.000	1050.000	-70.00	-270.60	62.00	-138.60	200.60
7	6000.000	900.000	-140.00	-454.54	-6.00	-320.54	314.54
8	7000.000	860.000	-150.00	-542.18	-14.00	-406.18	392.18
9	8000.000	800.000	-85.00	-405.41	53.00	-267.41	320.41
10	9000.000	750.000	30.00	-170.86	170.00	-30.86	200.86
11	10000.000	700.000	120.00	70.33	262.00	212.33	49.67
12	11000.000	600.000	300.00	337.04	444.00	481.04	-37.04
13	12000.000	500.000	440.00	555.53	586.00	701.53	-115.53
14	13000.000	420.000	330.00	445.59	478.00	593.59	-115.59
15	14000.000	425.000	205.00	261.92	355.00	411.92	-56.92
16	15000.000	435.000	95.00	137.05	247.00	289.05	-42.05
17	16000.000	430.000	0.00	56.97	154.00	210.97	-56.97
18	17000.000	420.000	-100.00	3.56	56.00	159.56	-103.56
19	18000.000	420.000	-120.00	-33.37	38.00	124.63	-86.63
20	19000.000	420.000	-140.00	-59.92	20.00	100.08	-80.08

* Model Data *

Background susceptibility = 0.00000

Polygon no. 1 Susceptibility = 0.00100
Strike half length = 20000.000

X-vertice	Z-vertice
-15000.000	0.000
13000.000	0.000
19000.000	2200.000
25000.000	4000.000
33000.000	6000.000
-15000.000	6000.000
-15000.000	0.000

Polygon no. 2 Susceptibility = 0.00500

Strike half length = 7000.00000

X-vertice	Z-vertice
-7000.000	0.000
~~2700.000~~	0.000
~~2700.000~~	5000.000
-7000.000	5000.000
-7000.000	0.000

Polygon no. 3 Susceptibility = 0.01000
Strike half length = 12000.000

X-vertice	Z-vertice
7000.000	500.000
12000.000	500.000
12000.000	5000.000
~~7000.000~~	5000.000
7000.000	500.000

* Regional Data *

Left regional - X = -1000.000
Left regional - mag.intens. = -120.000
Right regional - X = 19000.000
Right regional - mag.intens. = -160.000

Regional values for current station locations

	Station dis.	Regional
1	0.000	-122.000
2	1000.000	-124.000
3	2000.000	-126.000
4	3000.000	-128.000
5	4000.000	-130.000
6	5000.000	-132.000
7	6000.000	-134.000
8	7000.000	-136.000
9	8000.000	-138.000
10	9000.000	-140.000
11	10000.000	-142.000
12	11000.000	-144.000
13	12000.000	-146.000
14	13000.000	-148.000
15	14000.000	-150.000
16	15000.000	-152.000
17	16000.000	-154.000
18	17000.000	-156.000
19	18000.000	-158.000
20	19000.000	-160.000

INPUT PARAMETERS FOR FIGURES IN TEXT

Figure 4b, Transverse fault	3-D
Figure 4c, Rift zone and dikes	3-D
Figure 5a, Lae O Kahuna Coast Profile #1	2 1/2-D
Figure 5b, Lae O Kahuna Coast Profile #1	2 1/2-D
Figure 5c, Line 41, S. Coastline Area, Profile #2	2 1/2-D
Figure 5d, Line 41, S. Coastline Area, Profile #2	2 1/2-D
Figure 8 Puu Kaliu Rift, L-36-L-39	2 1/2-D

'roject name: T-FAULT

Model: MODEL 1

Figure 4b

Jnits in Feet

IAGNETIC PARAMETERS
:arth"s field: 35850. gammas.
Inclination = 37. degrees Declination = 11. degrees.

'RISM	X1	X2	Y1	Y2	D1	D2	DC	SC
1	-15000.	-6020.	8020.	9800.	2000.	4000.	0.00	5000.
2	-14000.	-4800.	7020.	8020.	2000.	4000.	0.00	5000.
3	-13000.	-4200.	6020.	7020.	2000.	4000.	0.00	5000.
4	-12000.	-3470.	5020.	6020.	2000.	4000.	0.00	5000.
5	-11000.	-2750.	4020.	5020.	2000.	4000.	0.00	5000.
6	-10000.	-2100.	3020.	4020.	2000.	4000.	0.00	5000.
7	-10000.	-1400.	2020.	3020.	2000.	4000.	0.00	5000.
8	-10000.	-650.	1020.	2020.	2000.	4000.	0.00	5000.
9	-10000.	50.	20.	1020.	2000.	4000.	0.00	5000.
10	-10000.	700.	-1020.	20.	1000.	3000.	0.00	5000.
11	-9800.	1400.	-2020.	-1020.	1000.	3000.	0.00	5000.
12	-9100.	2150.	-3020.	-2020.	1000.	3000.	0.00	5000.
13	-8300.	2900.	-4020.	-3020.	1000.	3000.	0.00	5000.
14	-7800.	3600.	-5020.	-4020.	1000.	3000.	0.00	5000.
15	-7100.	4300.	-6020.	-5020.	1000.	3000.	0.00	5000.
16	-6200.	5200.	-7200.	-6020.	1000.	3000.	0.00	5000.
17	-5050.	6400.	-10000.	-7200.	1000.	3000.	0.00	5000.

GRID PARAMETERS
Magnetic Model
Number of Grid Points in X Direction: 17

Project name: RIFT ZONE & DIKES

Model: MODEL 3

Figure 4c

Units in Feet

MAGNETIC PARAMETERS
Earth"s field: 35850. gammas.
Inclination = 37. degrees Declination = 11. degrees.

PRISM	X1	X2	Y1	Y2	D1	D2	DC	SC
1	-8020.	-4020.	-6400.	-5020.	1500.	5500.	0.00	5000.
2	-7020.	-3020.	-5020.	-4020.	1500.	5500.	0.00	5000.
3	-5020.	-1020.	-4020.	-2800.	1500.	5500.	0.00	5000.
4	-3250.	750.	-2800.	-1600.	1500.	5500.	0.00	5000.
5	-1820.	2200.	-1600.	-600.	1500.	5500.	0.00	5000.
6	-520.	3520.	-600.	400.	2500.	6500.	0.00	5000.
7	900.	4900.	400.	1400.	2500.	6500.	0.00	5000.
8	2100.	6100.	1400.	2400.	2500.	6500.	0.00	5000.
9	3520.	7520.	2400.	3400.	2500.	6500.	0.00	5000.
10	4700.	8700.	3400.	4400.	2500.	6500.	0.00	5000.

GRID PARAMETERS
Magnetic Model
Number of Grid Points in X Direction: 19
Number of Grid Points in Y Direction: 19
Grid Spacing in Feet: 1000.00
X Offset in Feet: 0.00
Y Offset in Feet: 0.00

Work File Header: ROSS
Earth's total magnetic field (gammas) = 35850.000
Inclination (deg.) of earth's total field = 37.0000
Angle (deg.) from magnetic north to profile axis = 124.0000

NOTE: The printed results are from a previous model
This model has not been executed

The total sum of squares is 20522.258
Units of distance for this model = FEET
Meters per unit of distance = 0.305
Number of inches per unit of distance = 12.000
The Current map scale is set to 1.

* Station Data *

Profile Id: LAE O'KAHUNA COAST PROFILE #1 Fig. 5a

Station	Distance to Station	Elev.	Observed Magnetic	Calc. Magnetic	Anomaly	Total Magnetic	Diff. ANM-MAG
1	0.000	600.000	-150.00	-166.09	50.00	33.91	16.09
2	1000.000	590.000	-175.00	-178.74	41.67	37.92	3.74
3	2000.000	610.000	-209.00	-210.98	24.33	22.35	1.98
4	3000.000	580.000	-240.00	-252.42	10.00	-2.42	12.42
5	4000.000	570.000	-288.00	-300.82	-21.33	-34.15	12.82
6	5000.000	550.000	-340.00	-345.39	-56.67	-62.06	5.39
7	6000.000	550.000	-310.00	-351.17	-10.00	-51.17	41.17
8	7000.000	545.000	-185.00	-256.44	131.67	60.23	71.44
9	8000.000	550.000	-27.00	-49.89	306.33	283.45	22.89
10	9000.000	520.000	170.00	199.20	520.00	549.20	-29.20
11	10000.000	560.000	217.00	211.20	583.67	577.86	5.80
12	11000.000	570.000	0.00	-21.13	383.33	362.20	21.13
13	12000.000	580.000	-150.00	-161.76	250.00	238.24	11.76
14	13000.000	580.000	-220.00	-243.82	196.67	172.85	23.82
15	14000.000	580.000	-290.00	-301.55	143.33	131.78	11.55
16	15000.000	580.000	-340.00	-348.54	110.00	101.46	8.54
17	16000.000	580.000	-378.00	-386.95	88.67	79.72	8.95
18	17000.000	580.000	-397.00	-418.59	86.33	64.75	21.59
19	18000.000	580.000	-409.00	-445.74	91.00	54.26	36.74
20	19000.000	580.000	-415.00	-470.27	101.67	46.40	55.27
21	20000.000	580.000	-420.00	-493.35	113.33	39.98	73.35

* Model Data *

Background susceptibility = 0.00000

Polygon no. 1 Susceptibility = 0.00175
Strike half length = $10000.000

X-vertice	Z-vertice
10000.000	0.000
13300.000	1000.000
15400.000	2300.000
17000.000	2950.000
18000.000	3300.000
26000.000	7000.000
-20000.000	7000.000
-20000.000	0.000

10000.000	0.000

Polygon no. 2 Susceptibility = 0.01100
Strike half length = $10000.000

X-vertice	Z-vertice
7000.000	900.000
9700.000	200.000
8000.000	5200.000
-10000.000	5200.000
-10000.000	3000.000
0.000	3000.000
4800.000	3000.000
7000.000	900.000

Polygon no. 3 Susceptibility = 0.00185
Strike half length = 5000.00000

Fig. 5a

X-vertice	Z-vertice
-10000.000	500.000
0.000	500.000
4800.000	3000.000
0.000	3000.000
-10000.000	3000.000
-10000.000	500.000

* Regional Data *

Left regional - X = 0.000
Left regional - mag.intens. = -200.000
Right regional - X = 18000.000
Right regional - mag.intens. = -500.000

Regional values for current station locations

	Station dis.	Regional
1	0.000	-200.000
2	1000.000	-216.667
3	2000.000	-233.333
4	3000.000	-250.000
5	4000.000	-266.667
6	5000.000	-283.333
7	6000.000	-300.000
8	7000.000	-316.667
9	8000.000	-333.333
10	9000.000	-350.000
11	10000.000	-366.667
12	11000.000	-383.333
13	12000.000	-400.000
14	13000.000	-416.667
15	14000.000	-433.333
16	15000.000	-450.000
17	16000.000	-466.667
18	17000.000	-483.333
19	18000.000	-500.000
20	19000.000	-516.667
21	20000.000	-533.333

Work File Header: ROSS
orth's total magnetic field (gammas) = 35850.000
Inclination (deg.) of earth's total field = 37.0000
Angle (deg.) from magnetic north to profile axis = 124.0000

)TE: The printed results are from a previous model
This model has not been executed

ne total sum of squares is 499794.563
nits of distance for this model = FEET
Meters per unit of distance = 0.305
umber of inches per unit of distance = 12.000
ne Current map scale is set to 1.

* Station Data *

Profile Id: LAE O'KAHUNA COAST PROFILE #1 Fig.5b

Station	Distance to Station	Elev.	Observed Magnetic	Calc. Magnetic	Anomaly	Total Magnetic	Diff. ANM-MAG
1	0.000	600.000	-150.00	-154.81	50.00	45.19	4.81
2	1000.000	590.000	-175.00	-162.99	41.67	53.68	-12.01
3	2000.000	610.000	-209.00	-184.86	24.33	48.47	-24.14
4	3000.000	580.000	-240.00	-208.16	10.00	41.84	-31.84
5	4000.000	570.000	-288.00	-230.77	-21.33	35.90	-57.23
6	5000.000	550.000	-340.00	-250.77	-56.67	32.57	-89.23
7	6000.000	550.000	-310.00	-266.24	-10.00	33.76	-43.76
8	7000.000	545.000	-185.00	-275.83	131.67	40.84	90.83
9	8000.000	550.000	-27.00	-277.01	306.33	56.32	250.01
10	9000.000	520.000	170.00	-262.47	520.00	87.53	432.47
11	10000.000	560.000	217.00	-199.79	583.67	166.88	416.79
12	11000.000	570.000	0.00	-181.79	383.33	201.54	181.79
13	12000.000	580.000	-150.00	-195.42	250.00	204.58	45.42
14	13000.000	580.000	-220.00	-208.43	196.67	208.23	-11.57
15	14000.000	580.000	-290.00	-232.98	143.33	200.36	-57.02
16	15000.000	580.000	-340.00	-270.13	110.00	179.87	-69.87
17	16000.000	580.000	-378.00	-307.54	88.67	159.13	-70.46
18	17000.000	580.000	-397.00	-340.52	86.33	142.81	-56.48
19	18000.000	580.000	-409.00	-369.94	91.00	130.06	-39.06
20	19000.000	580.000	-415.00	-397.76	101.67	118.91	-17.24
21	20000.000	580.000	-420.00	-425.29	113.33	108.04	5.29

* Model Data *

background susceptibility = 0.00000

Polygon no. 1 Susceptibility = 0.00500
Strike half length = 110000.000

X-vertice	Z-vertice
10000.000	0.000
13300.000	1000.000
15400.000	2300.000
17000.000	2950.000
18000.000	3300.000
26000.000	7000.000
-20000.000	7000.000
-20000.000	0.000

10000.000	0.000

Polygon no. 2 Susceptibility = 0.00185
Strike half length = 5000.00000

X-vertice	Z-vertice
-10000.000	500.000
0.000	500.000
4800.000	3000.000
0.000	3000.000
-10000.000	3000.000
-10000.000	500.000

* Regional Data *

Fig. 5b

Left regional - X = 0.000
Left regional - mag.intens. = -200.000
Right regional - X = 18000.000
Right regional - mag.intens. = -500.000

Regional values for current station locations

	Station dis.	Regional
1	0.000	-200.000
2	1000.000	-216.667
3	2000.000	-233.333
4	3000.000	-250.000
5	4000.000	-266.667
6	5000.000	-283.333
7	6000.000	-300.000
8	7000.000	-316.667
9	8000.000	-333.333
10	9000.000	-350.000
11	10000.000	-366.667
12	11000.000	-383.333
13	12000.000	-400.000
14	13000.000	-416.667
15	14000.000	-433.333
16	15000.000	-450.000
17	16000.000	-466.667
18	17000.000	-483.333
19	18000.000	-500.000
20	19000.000	-516.667
21	20000.000	-533.333

F1

Work File Header: ROSS
Earth's total magnetic field (gammas) = 35850.000
Inclination (deg.) of earth's total field = 37.0000
Angle (deg.) from magnetic north to profile axis = 129.0000

NOTE: The printed results are from a previous model
This model has not been executed

The total sum of squares is 37960.945
Units of distance for this model = FEET
Meters per unit of distance = 0.305
Number of inches per unit of distance = 12.000
The Current map scale is set to 1.

* Station Data *

Profile Id: PROFILE #2,LINE 41 S.COASTLINE AREA Fig. 5c

Station	Distance to Station	Elev.	Observed Magnetic	Calc. Magnetic	Anomaly	Total Magnetic	Diff. ANM-MAG
1	0.000	645.000	80.00	73.51	124.44	117.95	6.49
2	500.000	615.000	60.00	65.79	115.56	121.35	-5.79
3	1000.000	593.000	50.00	57.57	116.67	124.24	-7.57
4	1500.000	580.000	40.00	44.50	117.78	122.28	-4.50
5	2000.000	545.000	30.00	22.71	118.89	111.60	7.29
6	2500.000	534.000	20.00	-15.01	120.00	84.99	35.01
7	3000.000	535.000	-30.00	-66.58	81.11	44.53	36.58
8	3500.000	534.000	-100.00	-124.86	22.22	-2.64	24.86
9	4000.000	530.000	-140.00	-183.22	-6.67	-49.89	43.22
10	4500.000	527.000	-210.00	-235.99	-65.56	-91.55	25.99
11	5000.000	522.000	-260.00	-278.30	-104.44	-122.75	18.30
12	5500.000	520.000	-270.00	-304.43	-103.33	-137.76	34.43
13	6000.000	510.000	-260.00	-311.30	-82.22	-133.52	51.30
14	6500.000	500.000	-240.00	-295.43	-51.11	-106.54	55.43
15	7000.000	490.000	-214.00	-256.69	-14.00	-56.69	42.69
16	7500.000	480.000	-176.00	-195.50	35.11	15.61	19.50
17	8000.000	495.000	-105.00	-107.34	117.22	114.88	2.34
18	8500.000	500.000	-20.00	11.39	213.33	244.73	-31.39
19	9000.000	508.000	100.00	161.34	344.44	405.79	-61.34
20	9500.000	530.000	225.00	296.14	480.56	551.70	-71.14
21	10000.000	582.000	287.00	322.92	553.67	589.59	-35.92
22	10500.000	580.000	240.00	250.05	517.78	527.83	-10.05
23	11000.000	548.000	120.00	144.71	408.89	433.60	-24.71
24	11500.000	510.000	0.00	53.35	300.00	353.35	-53.35
25	12000.000	582.000	-80.00	-18.12	231.11	292.99	-61.88
26	12500.000	570.000	-120.00	-71.81	202.22	250.41	-48.19
27	13000.000	570.000	-145.00	-114.78	188.33	218.55	-30.22
28	13500.000	575.000	-170.00	-150.36	174.44	194.08	-19.64
29	14000.000	580.000	-193.00	-180.84	162.56	174.72	-12.16
30	14500.000	575.000	-218.00	-207.70	148.67	158.97	-10.30
31	15000.000	575.000	-240.00	-231.93	137.78	145.85	-8.07
32	15500.000	585.000	-265.00	-254.34	123.89	134.55	-10.66
33	16000.000	590.000	-283.00	-275.55	117.00	124.45	-7.45

* Model Data *

Background susceptibility = 0.00000

Polygon no. 1 Susceptibility = 0.00175
Strike half length = $20000.000

X-vertice	Z-vertice
-20000.000	0.000
10000.000	0.000
13000.000	1000.000
15000.000	1800.000
16000.000	2300.000
22000.000	6500.000
-10000.000	6500.000
-20000.000	0.000

Polygon no. 2 Susceptibility = 0.00600
Strike half length = $10000.000

X-vertice	Z-vertice
-11000.000	500.000
-3000.000	500.000
-3000.000	6000.000
-11000.000	6000.000
-11000.000	500.000

Polygon no. 3 Susceptibility = 0.01100
Strike half length = $10000.000

X-vertice	Z-vertice
3850.000	500.000
10000.000	300.000
7000.000	6500.000
5000.000	6500.000
5850.000	2000.000
8850.000	500.000

Polygon no. 4 Susceptibility = 0.00450
Strike half length = $10000.000

X-vertice	Z-vertice
-3000.000	1250.000
2250.000	1250.000
2250.000	6500.000
0.000	6500.000
-3000.000	6500.000
-3000.000	1000.000

Fig. 5c

* Regional Data *

Left regional - X = -2000.000
Left regional - mag.intens. = 0.000
Right regional - X = 10000.000
Right regional - mag.intens. = -400.000

Regional values for current station locations

	Station dis.	Regional
1	0.000	-44.444
2	500.000	-55.556
3	1000.000	-66.667

Work File Header: ROSS
arth's total magnetic field (gammas) = 35850.000
Inclination (deg.) of earth's total field = 37.0000
Angle (deg.) from magnetic north to profile axis = 129.0000

OTE: The printed results are from a previous model
This model has not been executed

he total sum of squares is 647284.375
Units of distance for this model = FEET
Meters per unit of distance = 0.305
umber of inches per unit of distance = 12.000
he Current map scale is set to 1.

* Station Data *

Profile Id: PROFILE #2,LINE 41 S,COASTLINE AREA Fig.5d

Station	Distance to Station	Elev.	Observed Magnetic	Calc. Magnetic	Anomaly	Total Magnetic	Diff. ANM-MAG
1	0.000	645.000	80.00	131.80	124.44	176.24	-51.80
2	500.000	615.000	60.00	111.03	115.56	166.58	-51.03
3	1000.000	593.000	50.00	93.87	116.67	160.54	-43.87
4	1500.000	580.000	40.00	78.36	117.78	156.14	-38.36
5	2000.000	545.000	30.00	62.63	118.89	151.52	-32.63
6	2500.000	534.000	20.00	44.07	120.00	144.07	-24.07
7	3000.000	535.000	-30.00	22.85	81.11	133.96	-52.85
8	3500.000	534.000	-100.00	0.83	22.22	123.05	-100.83
9	4000.000	530.000	-140.00	-20.40	-6.67	112.94	-119.60
10	4500.000	527.000	-210.00	-39.96	-65.56	104.49	-170.04
11	5000.000	522.000	-260.00	-57.56	-104.44	98.00	-202.44
12	5500.000	520.000	-270.00	-73.12	-103.33	93.55	-196.88
13	6000.000	510.000	-260.00	-66.82	-82.22	90.96	-173.18
14	6500.000	500.000	-240.00	-98.58	-51.11	90.31	-141.42
15	7000.000	490.000	-214.00	-108.31	-14.00	91.69	-105.69
16	7500.000	480.000	-176.00	-115.74	35.11	95.37	-60.26
17	8000.000	495.000	-105.00	-119.62	117.22	102.60	14.62
18	8500.000	500.000	-20.00	-119.40	213.33	113.93	99.40
19	9000.000	508.000	100.00	-111.63	344.44	132.82	211.63
20	9500.000	530.000	225.00	-88.26	480.56	167.30	313.26
21	10000.000	582.000	287.00	-46.01	553.67	220.66	333.01
22	10500.000	580.000	240.00	-22.52	517.78	255.26	262.52
23	11000.000	548.000	120.00	-23.97	408.89	264.92	143.97
24	11500.000	510.000	0.00	-33.48	300.00	266.52	33.48
25	12000.000	582.000	-60.00	-48.71	231.11	262.40	-31.29
26	12500.000	570.000	-120.00	-59.92	202.22	262.31	-60.08
27	13000.000	570.000	-145.00	-71.47	188.33	261.87	-73.53
28	13500.000	575.000	-170.00	-83.69	174.44	260.75	-86.31
29	14000.000	580.000	-193.00	-96.79	162.56	258.76	-96.21
30	14500.000	575.000	-218.00	-110.50	148.67	256.17	-107.50
31	15000.000	575.000	-240.00	-125.46	137.78	252.32	-114.54
32	15500.000	585.000	-265.00	-142.11	123.89	246.78	-122.89
33	16000.000	590.000	-283.00	-160.17	117.00	239.83	-122.83

* Model Data *

Background susceptibility = 0.00000

Polygon no. 1 Susceptibility = 0.00500
Strike half length = $20000.000

X-vertice	Z-vertice
-20000.000	0.000
10000.000	0.000
13000.000	1000.000
15000.000	1800.000
16000.000	2300.000
22000.000	6500.000
-10000.000	6500.000
-20000.000	0.000

Polygon no. 2 Susceptibility = 0.00600
Strike half length = $10000.000

X-vertice	Z-vertice
-11000.000	500.000
-3000.000	500.000
-3000.000	6000.000
-11000.000	6000.000
-11000.000	500.000

Fig. 5d

Polygon no. 3 Susceptibility = 0.00150
Strike half length = $10000.000

X-vertice	Z-vertice
-3000.000	1250.000
2250.000	1250.000
2250.000	6500.000
0.000	6500.000
-3000.000	6500.000
-3000.000	1250.000

* Regional Data *

Left regional - X = -2000.000
Left regional - mag.intens. = 0.000
Right regional - X = 16000.000
Right regional - mag.intens. = -400.000

Regional values for current station locations

	Station dis.	Regional
1	0.000	-44.444
2	500.000	-55.556
3	1000.000	-66.667
4	1500.000	-77.778
5	2000.000	-88.889
6	2500.000	-100.000
7	3000.000	-111.111
8	3500.000	-122.222
9	4000.000	-133.333
10	4500.000	-144.444
11	5000.000	-155.556
12	5500.000	-166.667
13	6000.000	-177.778
14	6500.000	-188.889

F 14

Work File Header: ROSS
Earth's total magnetic field (gammas) = 35850.000
Inclination (deg.) of earth's total field = 37.0000
Angle (deg.) from magnetic north to profile axis = 129.0000

NOTE: The printed results are from a previous model
This model has not been executed

The total sum of squares is 62148.430
Units of distance for this model = FEET
Meters per unit of distance = 0.305
Number of inches per unit of distance = 12.000
The Current map scale is set to 1.

* Station Data *

Profile Id: PUU KALIU RIFT, L36-L39, PROFILE #3 Fig. 8

Station	Distance to Station	Elev.	Observed Magnetic	Calc. Magnetic	Anomaly	Total Magnetic	Diff. ANM-MAG
1	0.000	500.000	-20.00	-97.88	80.00	2.12	77.88
2	500.000	500.000	-100.00	-133.73	5.24	-28.50	33.73
3	1000.000	500.000	-190.00	-181.68	-79.52	-71.20	-8.32
4	1500.000	500.000	-240.00	-224.24	-124.29	-108.53	-15.76
5	2000.000	500.000	-250.00	-259.43	-129.05	-138.48	9.43
6	2500.000	500.000	-250.00	-290.36	-123.81	-164.17	40.36
7	3000.000	500.000	-280.00	-320.51	-148.57	-189.08	40.51
8	3500.000	500.000	-340.00	-352.47	-203.33	-215.80	12.47
9	4000.000	500.000	-400.00	-387.68	-258.10	-245.78	-12.32
10	4500.000	500.000	-425.00	-426.82	-277.86	-279.68	1.82
11	5000.000	500.000	-480.00	-470.12	-327.62	-317.74	-9.88
12	5500.000	500.000	-515.00	-517.35	-357.38	-359.73	2.35
13	6000.000	500.000	-550.00	-567.36	-387.14	-404.51	17.36
14	6500.000	500.000	-580.00	-617.25	-411.90	-449.15	37.25
15	7000.000	500.000	-605.00	-660.55	-431.67	-487.22	55.55
16	7500.000	510.000	-605.00	-679.62	-426.43	-501.05	74.62
17	8000.000	510.000	-560.00	-648.58	-376.19	-464.77	88.58
18	8500.000	520.000	-450.00	-519.32	-260.95	-330.27	69.32
19	9000.000	530.000	-320.00	-317.69	-125.71	-123.40	-2.31
20	9500.000	535.000	-160.00	-119.23	39.52	80.29	-40.77
21	10000.000	570.000	50.00	49.31	254.76	254.07	0.69
22	10500.000	600.000	250.00	197.40	460.00	407.40	52.60
23	11000.000	660.000	420.00	329.09	635.24	544.33	90.91
24	11500.000	700.000	500.00	450.96	720.48	671.43	49.04
25	12000.000	720.000	560.00	551.58	785.71	777.30	8.42
26	12500.000	750.000	590.00	591.29	820.95	822.24	-1.29
27	13000.000	700.000	560.00	583.39	796.19	819.58	-23.39
28	13500.000	610.000	500.00	521.18	741.43	762.61	-21.18
29	14000.000	565.000	400.00	419.16	646.67	665.83	-19.16
30	14500.000	560.000	305.00	315.22	556.90	567.12	-10.22
31	15000.000	540.000	230.00	224.83	487.14	481.97	5.17
32	15500.000	520.000	140.00	146.27	402.38	408.65	-6.27
33	16000.000	525.000	80.00	78.36	347.62	345.98	1.64
34	16500.000	535.000	20.00	20.43	292.86	293.29	-0.43
35	17000.000	545.000	-40.00	-29.05	238.10	249.05	-10.95
36	17500.000	550.000	-70.00	-71.51	213.33	211.83	1.51
37	18000.000	560.000	-100.00	-107.95	188.57	180.63	7.95
38	18500.000	530.000	-140.00	-140.10	153.81	153.71	0.10

39	19000.000	530.000	-200.00	-167.52	99.05	131.52	-32.48
40	19500.000	530.000	-240.00	-191.39	64.29	112.90	-48.61
41	20000.000	530.000	-260.00	-212.25	49.52	97.27	-47.75
42	20500.000	530.000	-280.00	-230.60	34.76	84.16	-49.40
43	21000.000	530.000	-300.00	-246.82	20.00	73.18	-53.18

* Model Data *

Background susceptibility = 0.00000

Polygon no. 1 Susceptibility = 0.00200
Strike half length = $10000.000

X-vertice	Z-vertice
-20000.000	0.000
30000.000	0.000
46000.000	6600.000
-20000.000	6600.000
-20000.000	0.000

Fig. 8

Polygon no. 2 Susceptibility = 0.01200
Strike half length = $10000.000

X-vertice	Z-vertice
12000.000	500.000
12500.000	500.000
14500.000	6000.000
10000.000	6000.000
10750.000	2500.000
11000.000	1500.000
12000.000	500.000

Polygon no. 3 Susceptibility = 0.01400
Strike half length = $10000.000

X-vertice	Z-vertice
8500.000	500.000
12000.000	500.000
11000.000	1500.000
10750.000	2500.000
10000.000	6000.000
0.000	6000.000
0.000	4500.000
6000.000	3500.000
8500.000	500.000

Polygon no. 4 Susceptibility = 0.00250
Strike half length = $10000.000

X-vertice	Z-vertice
0.000	2000.000
3000.000	2000.000
3000.000	3000.000
6400.000	3000.000
6000.000	3500.000
0.000	4500.000
0.000	2000.000

Polygon no. 5 Susceptibility = 0.00400
Strike half length = $10000.000

X-vertice	Z-vertice
-10000.000	500.000
0.000	500.000
0.000	6000.000
-10000.000	6000.000
-10000.000	500.000

* Regional Data *

Fig. 8

Left regional - X = 0.000
Left regional - mag.intens. = -100.000
Right regional - X = 21000.000
Right regional - mag.intens. = -320.000

Regional values for current station locations

	Station dis.	Regional
1	0.000	-100.000
2	500.000	-105.238
3	1000.000	-110.476
4	1500.000	-115.714
5	2000.000	-120.952
6	2500.000	-126.190
7	3000.000	-131.429
8	3500.000	-136.667
9	4000.000	-141.905
10	4500.000	-147.143
11	5000.000	-152.381
12	5500.000	-157.619
13	6000.000	-162.857
14	6500.000	-168.095
15	7000.000	-173.333
16	7500.000	-178.571
17	8000.000	-183.810
18	8500.000	-189.048
19	9000.000	-194.286
20	9500.000	-199.524
21	10000.000	-204.762
22	10500.000	-210.000
23	11000.000	-215.238
24	11500.000	-220.476
25	12000.000	-225.714
26	12500.000	-230.952
27	13000.000	-236.190
28	13500.000	-241.429
29	14000.000	-246.667
30	14500.000	-251.905
31	15000.000	-257.143
32	15500.000	-262.381
33	16000.000	-267.619
34	16500.000	-272.857
35	17000.000	-278.095
36	17500.000	-283.333
37	18000.000	-288.571